NAVAL POSTGRADUATE SCHOOL
Monterey, California

THESIS

COASTAL EROSION ALONG MONTEREY BAY

by

Anastasios I. Sklavidis
and
Williams R. Lima Blanco

March 1985

Thesis Co-advisors: E. B. Thornton
S. P. Tucker

REPORT DOCUMENTATION PAGE

READ INSTRUCTIONS BEFORE COMPLETING FORM

1. REPORT NUMBER	2. GOVT ACCESSION NO. / 3. RECIPIENT'S CATALOG NUMBER
4. TITLE (and Subtitle): COASTAL EROSION ALONG MONTEREY BAY	5. TYPE OF REPORT & PERIOD COVERED: Master's thesis; March 1985
	6. PERFORMING ORG. REPORT NUMBER
7. AUTHOR(s): Anastasois I. Sklavidis and Williams R. Lima Blanco	8. CONTRACT OR GRANT NUMBER(s)
9. PERFORMING ORGANIZATION NAME AND ADDRESS: Naval Postgraduate School, Monterey, California 93943	10. PROGRAM ELEMENT, PROJECT, TASK AREA & WORK UNIT NUMBERS
11. CONTROLLING OFFICE NAME AND ADDRESS: Naval Postgraduate School, Monterey, California 93943	12. REPORT DATE: March 1985 / 13. NUMBER OF PAGES: 107
14. MONITORING AGENCY NAME & ADDRESS (if different from Controlling Office): Naval Postgraduate School, Monterey, California 93943	15. SECURITY CLASS. (of this report): UNCLASSIFIED / 15a. DECLASSIFICATION/ DOWNGRADING SCHEDULE

16. DISTRIBUTION STATEMENT (of this Report)

Approved for public release; distribution unlimited.

17. DISTRIBUTION STATEMENT (of the abstract entered in Block 20, if different from Report)

18. SUPPLEMENTARY NOTES

19. KEY WORDS (Continue on reverse side if necessary and identify by block number)

Erosion
Top of the Cliff
Refraction
Wave Run-up
Wave Set-up
Tide Height

20. ABSTRACT (Continue on reverse side if necessary and identify by block number)

The permanent beach erosion in Southern Monterey Bay is episodic, occurring infrequently when high tides coincide with stormy weather which allows wave action to erode the toe of the cliffs. Precise photogrammetric techniques are used to measure cliff recession from 1946 through 1984. This study shows maximum erosion occurs in the vicinity of Fort Ord (7.3 ft/yr) and decreases to the south. The analysis and errors associated with determining cliff recession using aerial photogrammetry are discussed in detail.

A model is developed to predict cliff erosion based on the hypothesis that erosion only occurs when the water level due to combined tides, wave set-up and run-up exceeds the toe of the cliff elevation. The model combines predicted tidal elevations and wave heights. Shallow water wave heights at various locations are calculated by transforming deep-water directional wave spectra provided by the Fleet Numerical Oceanography Center. Refraction of the wave energy is responsible for the variability of erosion rates along the shore. The bathymetry of Monterey Bay is such that the refracted wave energy is greater in the Fort Ord area than to the south. The erosion model was calibrated using the spectral wave climatology and aerial photographs covering an 18 year period. The model qualitatively replicates the temporal variability of the measured recession rates and gives a reasonable prediction of the spatial variation of the mean recession rates.

Coastal Erosion Along Monterey Bay

by

Anastasios I. Sklavidis
Lieutenant, Hellenic Navy
B.S., Naval Academy of Greece, 1973

and

Williams R. Lima Blanco
Lieutenant Commander, Venezuelan Navy
B.S., Naval Academy of Venezuela, 1971

Submitted in partial fulfillment of the
requirements for the degree of

MASTER OF SCIENCE IN HYDROGRAPHIC SCIENCE

from the

NAVAL POSTGRADUATE SCHOOL
March 1985

ABSTRACT

The permanent beach erosion in Southern Monterey Bay is episodic, occurring infrequently when high tides coincide with stormy weather which allows wave action to erode the toe of the cliffs. Precise photogrammetric techniques are used to measure cliff recession from 1946 through 1984. This study shows maximun erosion occurs in the vicinity of Fort Ord (7.3 ft/yr) and decreases to the south. The analysis and errors associated with determining cliff recession using aerial photogrammetry are discussed in detail.

A model is developed to predict cliff erosion based on the hypothesis that erosion only occurs when the water level due to combined tides, wave set-up and run-up exceeds the toe of the cliff elevation. The model combines predicted tidal elevations and wave heights. Shallow water wave heights at various locations are calculated by transforming deep-water directional wave spectra provided by the Fleet Numerical Oceanography Center. Refraction of the wave energy is responsible for the variability of erosion rates along the shore. The bathymetry of Monterey Bay is such that the refracted wave energy is greater in the Fort Ord area than to the south. The erosion model was calibrated using the spectral wave climatology and aerial photographs covering an 18 year period. The model qualitatively replicates the temporal variability of the measured recession rates and gives a reasonable prediction of the spatial variation of the mean recession rates.

TABLE OF CONTENTS

I. INTRODUCTION 11
A. NEEDS FOR AND USE OF COASTAL EROSION DATA . . 11
B. COASTAL EROSION PROCESS IN SOUTHERN MONTEREY BAY 12
C. EARLIER STUDIES OF COASTAL EROSION IN SOUTHERN MONTEREY BAY 17
D. OBJECTIVES 19

II. EROSION RATES MEASURED USING PHOTOGRAMMETRY . . . 20
A. METHODS FOR DETERMINING COASTAL EROSION . . . 20
B. ERROR CONSIDERATIONS IN UTILIZING AERIAL PHOTOGRAPHS 23
1. Scale Variation Due to Change in Ground Elevation 23
2. Errors Due to Relief Displacement 27
3. Scale Variation Due to Tilt 30
C. DESCRIPTION OF RESEARCH PROCEDURE 31
1. Procedure to Select, Locate and Purchase Aerial Photographs 31
2. Selection and Description of Subject Areas 33
3. Selection of Reference Points 35
4. Selection of Measurement Points 35
5. Measurement Techniques 38
D. APPLICATION AND ANALYSIS OF COASTAL EROSION DATA 41
1. Presentation of Data 41
2. Fort Ord 41
3. Sand Dune 47

4. Phillips Petroleum Property 52
5. Beach Lab 55
6. Comparison with Earlier Studies and Comments 60

III. TIDES 63

IV. SEA AND SWELL RUN-UP 69
A. WAVE CLIMATOLOGY 69
B. WAVE TRANSFORMATION FROM DEEP TO SHALLOW WATER 70
C. WAVE SET-UP AND RUN-UP 80

V. PREDICTIVE BEACH EROSION MODEL 82
A. MODEL FOR BEACH PROFILE RESPONSE 82

VI. CONCLUSION 89

APPENDIX A: SCALE VARIATION DUE TO TILT 91

APPENDIX B: RECORDING OF DATA AND COMPUTER PROGRAMS . . 95

APPENDIX C: TIDE TABLES 97

APPENDIX D: HISTORIC OCEAN STORMS 100

LIST OF REFERENCES 103

INITIAL DISTRIBUTION LIST 105

LIST OF TABLES

1. Erosion Rate Results for Fort Ord (North Region) 45
2. Erosion Rate Results for Fort Ord (South Region) 46
3. Erosion Rate Results for Sand Dune (North Region) 50
4. Erosion Rate Results for Sand Dune (South Region) 51
5. Erosion Rate Results for Phillips Petroleum Property 54
6. Erosion Rate Results for Beach Lab (North Area) 58
7. Erosion Rate Results for Beach Lab (South Area) 59
8. Wave Refraction Coefficients (Ft. Ord Area) . . . 73
9. Wave Refraction Coefficients (Sand Dune Area) . . 74
10. Wave Refraction Coefficients (Phillip Petroleum Area) 75
11. Wave Refraction Coefficients (Beach Lab Area) . . 76
12. Characteristics of the Study Areas 87
13. Recession Rates given by the Model (ft/yr). . . . 88
14. Tidal Constituents for Monterey, California . . . 98
15. Calculated Constituent Terms for Monterey 99
16. Historic Ocean Storms (Monterey Bay) 101

LIST OF FIGURES

1.1 Monterey Bay 13
1.2 Sediment Transport Processes (Monterey Bay) 14
1.3 Wave Refraction Diagrams for Monterey Bay, (Wiegel, 1964) 16
1.4 Erosion Rate (feet/year), Measured Using Aerial Photographs to Determine Bluff Recession (after Thornton,1984) 18
2.1 Scale Variation 24
2.2 Relief Displacement on a Vertical Photograph . . . 28
2.3 Relief Displacement of a Point 29
2.4 Selected Areas of Study 34
2.5 Selected Measurement Points 36
2.6 Fort Ord (Southern Monterey Bay). 42
2.7 Fort Ord (North) 43
2.8 Fort Ord (South) 44
2.9 Sand Dune (Southern Monterey Bay) 47
2.10 Sand Dune (North) 48
2.11 Sand Dune (South) 49
2.12 Phillips Petroleum Property 52
2.13 Phillips Petroleum Property 53
2.14 Beach Lab (Southern Monterey Bay) 55
2.15 Beach Lab (North) 56
2.16 Beach Lab (South) 57
2.17 Average Recession Rates in Southern Monterey Bay 62
3.1 Typical Tidal Cycle for Monterey Bay 67
3.2 Tidal Anomalies 68
4.1 Wave Refraction Diagram (Direction: WNW , Period: 15 s) 77

4.2 Wave Refraction Diagram (Direction: WNW, Period: 25.70 s) 78
4.3 Change in Mean Water Level 81
5.1 Characteristics of the response Model 82
5.2 Comparison of Normalized Measured and Predicted Recession Rates 85
5.3 Measured vs. Predicted Recession Rates (1966-83) 86
A.1 Elements of Tilted Photographs 91
A.2 Scale Variation on Tilted Photograph 92
B.1 Recording Data Sheet 96

ACKNOWLEDGEMENTS

At the completion of this research the authors first wish to express their graditude as well as their personal sincere appreciation to Professors E.B. Thornton and S.P. Tucker and to Captain D.E. Puccini for their attentive assistance in all phases of this work.

Furthermore, we would like to express our sincere appreciation to:

Donna Burych, for help in the computer programming; Cdr. Glen Schaefer and Mr. James Cherry for their advice and assistance; and Mr. Stan Steven, Librarian of University of California, Santa Cruz, for procuring aerial photographs.

Williams Lima dedicates this thesis to his parents Asuncion and Eliseo for their spiritual support and to his beloved Diane Spry for guidance and assistance in all aspects.

Anastasios Sklavidis dedicates this thesis to his wife Evagelia, who has always encuraged and helped him during his efforts for education and continuous self improvement.

I. INTRODUCTION

A. NEEDS FOR AND USE OF COASTAL EROSION DATA

Most of the world's population is located in coastal areas, where the length of the world's coastline is about 448,000 km. Residential and commercial buildings are frequently constructed close to beaches without regard to future physical changes of the coastline. In certain locations the coastline is eroded by wave action. Often beach erosion leads to wave damage of coastal structures, which results in economic losses.

These coastline changes, which are due primarily to wave action, illustrate the need for obtaining erosion data which can be used for rational coastal planning. Knowledge of shoreline erosion rates is important for effective planning and design on low sandy shores and on shores attacked directly by large storm waves. In such cases coastal erosion can be severe and permanent. Coastal development that is planned and constructed with appropriate consideration given to coastal erosion is the most economical. The need for obtaining erosion data is especially important for planning the growth of undeveloped areas of coastline. Erosion data may be obtained by studying coastal processes and collecting data over a long period of time using nautical charts, topographic maps, aerial photography, historical and repetitive field measurements.

The southern shoreline of Monterey Bay, between the Salinas River and Monterey Harbor, is a sandy beach and backshore with dune fields. This shoreline represents one of the most scenic regions of Monterey county. Several structures have been built close to the shoreline without

apparent consideration of coastal erosion. For example, Stilwell Hall at Fort Ord was built 80 feet from the shoreline in 1946. It was necessary to construct a protective revetment in 1950; again in 1983, a temporary revetment had to be built after the shoreline had severely eroded. Similar problems have been confronted by the Ocean House apartments on Del Monte Beach where a temporary stone wall has been constructed to slow erosion. More importantly, there is considerable pressure to develop extensive sections of the coastline with new hotels, condominiums and apartments. Thus, for southern Monterey Bay , there is a critical need for understanding erosion processes.

B. COASTAL EROSION PROCESS IN SOUTHERN MONTEREY BAY

Beach erosion is a process which occurs naturally in regions where the sea level is rising, as has been occurring during the past century along much of the California coast. Coastal cliffs are a common landform along large sections of the geologically young California coast. The cliffs are the result of active erosion, which occurs periodically during stormy periods.

Monterey Bay, California's second largest, is semicircular and opens to the west. The bay is 12 miles wide in an east-west direction and 25 miles long in a north-south direction, (Figure 1.1). The outer limits of the bay floor correspond to the edge of the continental shelf. Monterey Bay cliffs consist of coarse sand which is highly susceptible to erosion from wave action and surface runoff.

The sediment transfer and deposition budget along the shoreline depends on a source of sand, such as the Salinas River discharge and cliff erosion sand transport down the coast by waves and currents, and losses of sand into the deep ocean, onto land, and to sand mining (see Figure 1.2) .

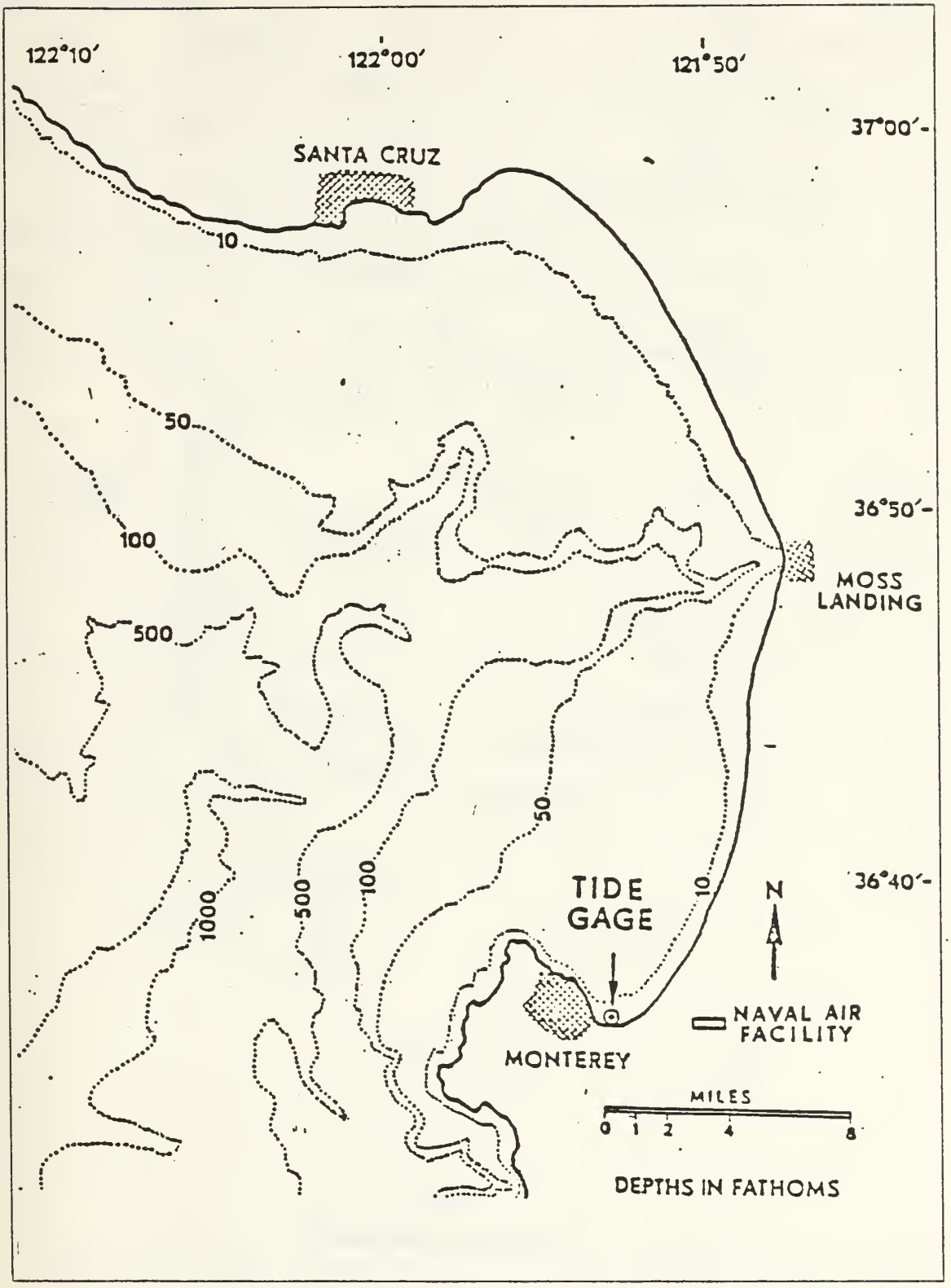

Figure 1.1 Monterey Bay

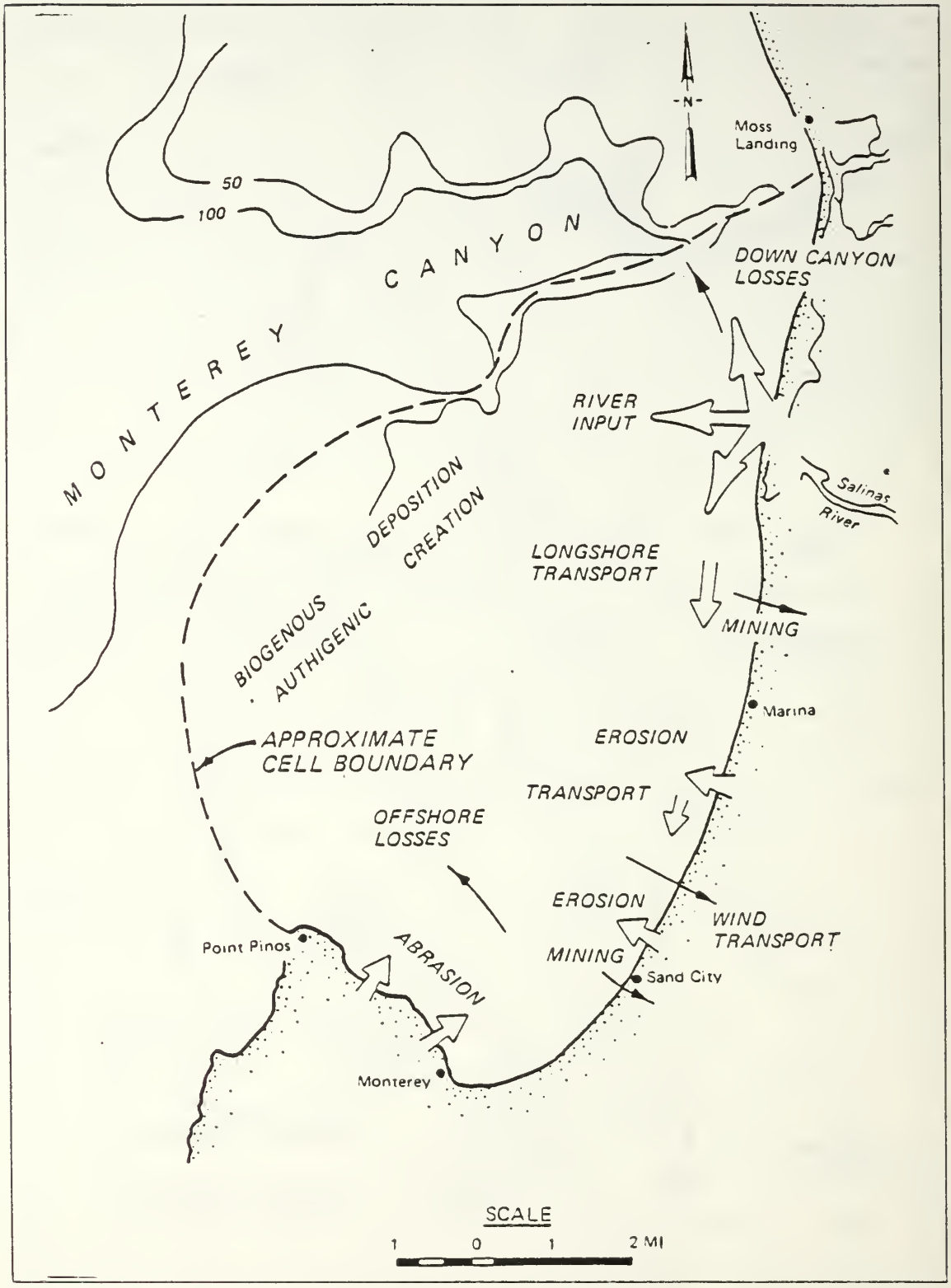

Figure 1.2 Sediment Transport Processes (Monterey Bay)

The difference between loss and gains determines whether there will be beach erosion or accretion. Studies conducted by Dorman (1968) and Arnal (1973) concluded that there is a net loss of sand, and therefore, a continuous erosion of Monterey Bay beaches.

The waves of Monterey Bay consist of both Pacific Ocean swells with periods of approximately 12-20 seconds and locally generated wind waves. Swells are the most significant sources of wave energy into the Bay. Early spring and summer are typically characterized by swells from the northwest, while fall and winter bring swells from west and southwest (Figure 1.2).

The distribution of sediments in Monterey Bay and its shoreline shape are in large part a response to wave climate. Sediment found near the shore, where wave effects at the bottom are stronger, tends to be coarser sand than that found offshore (Smith, 1983). Shorelines tend to orient themselves toward the waves that lead to the path of least resistance. The effect of the Monterey Bay bathymetry, anchored by rocky headlands at Point Pinos and Point Santa Cruz and perturbed by the Monterey Submarine Canyon, is to bend the wave-front into a shape approaching that of the shoreline shown in Figure 1.3 .

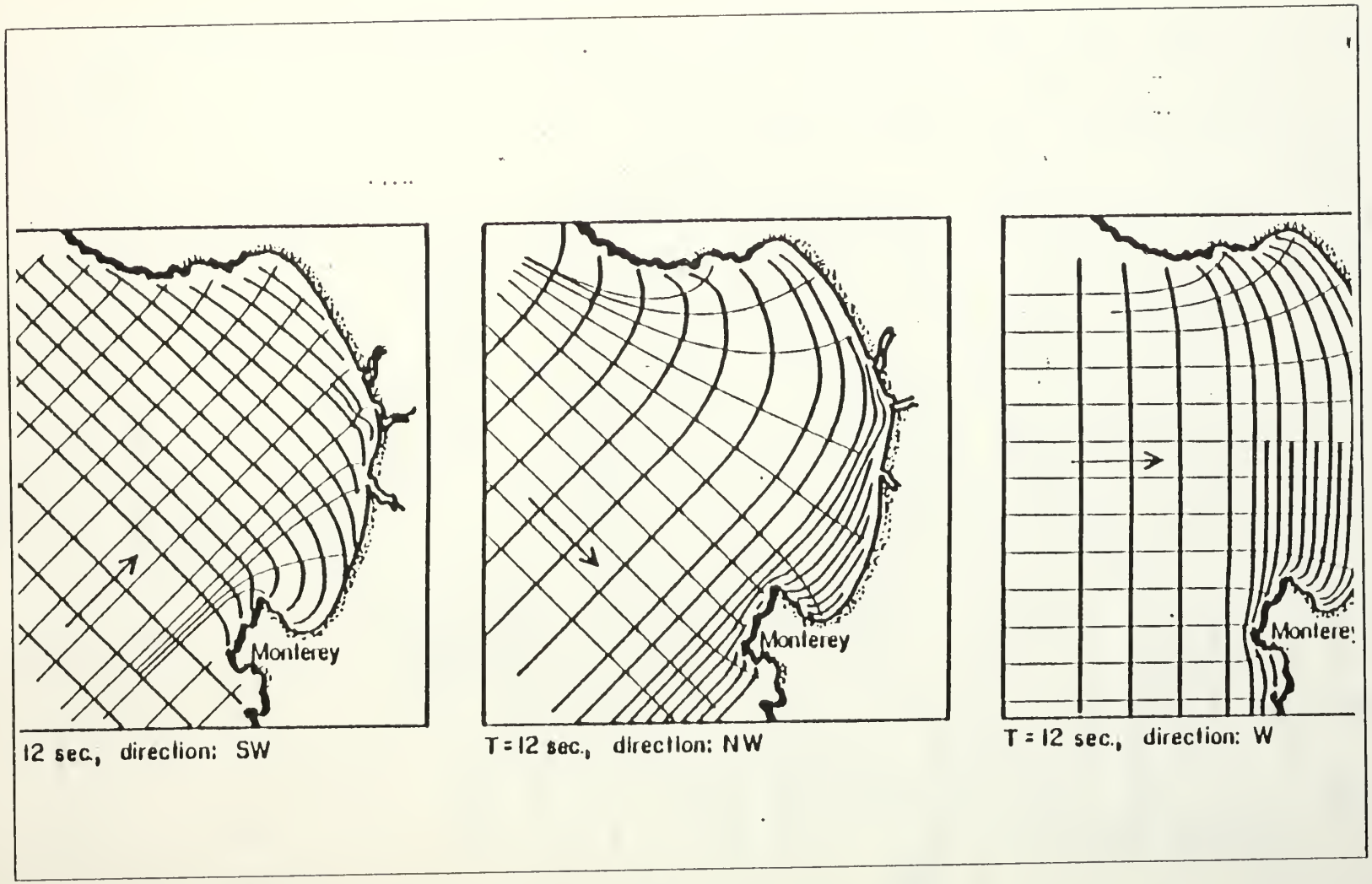

Figure 1.3 Wave Refraction Diagrams for Monterey Bay, (Wiegel, 1964)

C. EARLIER STUDIES OF COASTAL EROSION IN SOUTHERN MONTEREY BAY

Several coastal errosion studies have been conducted for Southern Monterey Bay; in general, they indicate a continuous erosion or recession of the coastal land. In most of these studies erosion is inferred by comparing shoreline changes measured from historical aerial photographs starting from the year 1939. Nautical charts from as far back as 1856 and topographical maps are used to complement photographs. Various reference points are selected for these studies to measure beach erosion, such as the top of the cliff, the toe of the coastal bluff, and the mean water line; selection of different reference points can lead to different measures of erosion rate.

One of the more significant studies for our purpose was performed by Thompson (1981), who obtained consistent estimates of erosion rates; he viewed aerial photographs with a mirror stereoscope to measure the recession of the toe of the cliff fronting the Phillips Petroleum Property. The average cliff recession rate between 1939 and 1978 was found to be 1.8 ft/yr (0.54 m/yr).

Moffitt (1968) used aerial photographs to determine the erosion rate at the Monterey Sand Company; the reference point used was the waterline. Since the waterline depends on tide elevation, waves, seasonal beach profile, referencing the waterline results in a "noisy" measure of erosion rate. The average erosion rate found was 6.9 ft/yr (2.1 m/yr) between 1946 and 1967. Other studies have been performed in the area, and the resultig erosion rates from these studies are summarized in Figure 1.4 .

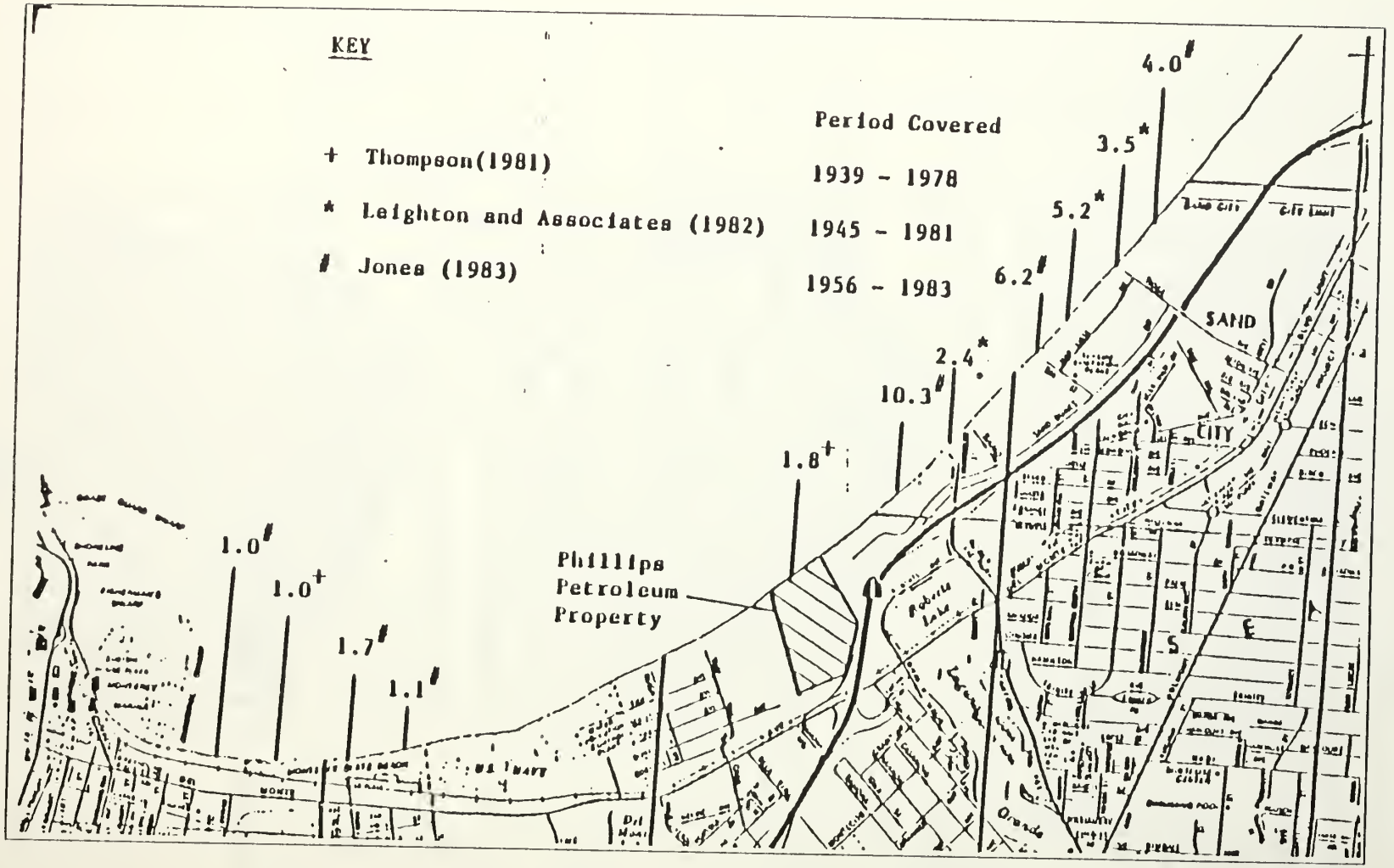

Figure 1.4 Erosion Rate (feet/year), Measured Using Aerial Photographs to Determine Bluff Recession (after Thornton,1984)

D. OBJECTIVES

The objective of the thesis is to construct a model to predict coastal changes due to stormy weather, taking into account the major contributions to the coastal erosion process. It is hypothesised that erosion is episodic and occurs during simultaneous occurrences of high tides and storm waves; thus, it is proposed that cliff erosion due to storms can be calculated, provided that local tide elevation, wave height, and a function relating storm energy and erosion are known.

The procedure followed is to obtain erosion rates using photogrammetry. Several of the previous erosion studies have utilized inprecise photo comparison techniques leading to erratic and questionable results. The precise photogrammetric techniques used here and associated errors are described in detail in Chapter II. The prediction of tides, the effect of waves and the various terms needed for studying coastal processes are explained in Chapters III and IV; and the model which is used for prediction of coastal changes is described in Chapter V.

II. EROSION RATES MEASURED USING PHOTOGRAMMETRY

A. METHODS FOR DETERMINING COASTAL EROSION

Beach erosion rates can be determined by several methods. The best method to be used depends on the available data and the objectives of the proposed survey. Erosion rates can be measured by comparison of historical data obtained through old maps and nautical charts. The charts and maps indicate the location of the shoreline at the date when the field measurements were taken before compiling the map. The change of shoreline is determined by comparing the shoreline on the charts at different times. Annual recession rates for a specific coast are determined by dividing the measured change of the shoreline by the time interval. Considering that the shoreline recession in southern Monterey Bay is nominally 3 ft/yr (0.9 m/yr) and that the accuracy of standard 1:24000 scale USGS topographic maps in horizontal positions is about 40 ft (0.5mm at scale), one would conclude that the measured recession rate using the above method is not accurate. Another problem is that the surveys for nautical charts are normally only made every fifty years in eighty percent of the areas concerned, and on five, ten, or twenty-five year cycles in the less stable areas that constitute the remaining twenty percent. Thus, only a small number of comparisons are available for most areas, with long time intervals between the possible charts (Stafford,1971).

Another method is to collect information for a specific beach through observations by local residents who have lived near the beach for long periods of time. Personal observation can provide valuable information about changes, but it

is the least reliable method for obtaining accurate erosion data and is not generally useful for engineering planning purposes. This method is normally only useful in areas that have been developed for a considerable length of time.

The most accurate method is to make repetitive profile surveys of the area of interest, utilizing permanent reference points on the beach. However, this method is time consuming and expensive because the surveys must be repeated many times at relatively short time intervals.

A less expensive alternative is to measure coastal erosion using aerial photographs. In the last four decades considerable progress has been made in photogrammetry. Charting agencies presently use aerial photographs to produce charts. This procedure reduces field work and the compilation time. By utilizing photogrammetric methods the charts can be revised more frequently, and the data is more accurate. The photography of identical areas at short intervals makes it possible to observe changes in the shoreline. By drawing the shoreline imaged on aerial photographs taken at different times, and comparing the drawn shorelines, coastal erosion rates may be estimated.

Before utilizing one of the above methods the first question to be answered is: What location is indicative of permanent beach change? For example, does one measure changes at the mean waterline, at the high tide line, at the base of the backshore cliff, or at the top of this cliff? This question will be discussed further in Subsection 2.D.4, where it is described that the cliff tops are the preferred reference points for this study.

The use of aerial photographs to determine shoreline changes has an advantage over other methods. For instance a permanent record of specific features, their location, and the contour of the shoreline are obtained in great detail at the time of the photography. All of the existing details of

the coast are recorded in the aerial photographs, while on topographic maps and nautical charts, details are limited by the purpose of the chart. For the purpose of measuring beach erosion, the aerial photograph permits a more comprehensive analysis than maps or charts. Features such as high water levels, cliffs, waterlines, waves, reference buildings, and roads are represented as a whole. In the last four decades governmental agencies such as the U.S. Coast and Geodetic Survey (USCGS), the National Ocean Service (NOS), the Defence Mapping Agency (DMA), and the U.S. Department of Agriculture (USDA) have been photographing the coasts more frequently than new maps or charts have been made. This allows the determination of coastal changes to be made more frequently and at relatively less cost than to produce a new map or chart (Stafford, 1971).

The coast of Southern Monterey Bay has been photographed at an average interval of about every five years since 1939. However, in the last decade the photographic interval has been shorter, about every three years, which allows a more precise determination of erosion rates and a clearer picture of coastal change. The process of taking the necessary aerial photographs is expensive; however, for this study, photographs were obtained from private and government agencies at relatively low cost ($150.00 per set). A disadvantage of the aerial photographic method is that aerial photographs are generally only available back to 1939.

Several errors may result from using aerial photography to measure coastal erosion. The most significant errors are:

a. Scale variation due to altitude variation of the airplane.

b. Scale variation due to ground elevation variation.

c. Horizontal displacement of the image due to relief.

d. Scale variation due to tilt of the camera.

A discussion of each of these errors is presented below.

B. ERROR CONSIDERATIONS IN UTILIZING AERIAL PHOTOGRAPHS

A map is a reproduction at reduced scale of an orthographic projection of the terrain onto a reference datum plane. Each point on the terrain is seen to be projected normal to the reference plane. A distance measured between two points on the map when multiplied by the scale of the map will be equal to the corresponding horizontal distance measured in the field.

A photo is a perspective or central projection. It is one in which all points are projected onto the reference plane through one point called the perspective center. A photo is only orthographic in the ideal case when the film and ground lie in parallel planes; therefore direct measurements on single photo may cause error (Moffitt, 1980). Because the study of coastal erosion requires very accurate shoreline determination, photogrammetric errors must be considered. The most important error inherent in photographs is the scale variation.

1. Scale Variation Due to Change in Ground Elevation

The exact scale of the photographs must be known in order to obtain accurate ground distances from aerial photographs. If ground distances are found by measuring photo distances on two different photographs and utilizing a nominal scale for the photographs , an apparent difference in ground distances can result where there is no actual difference. The scale, S, of a vertical aerial photograph, for a particular point is given by Equation 2.1 (Moffitt, 1980).

$$S = f/(H-h) \qquad (2.1)$$

where f is the focal length of the aerial camera's lens, H is the flight height above datum, and h is the ground elevation of the point.

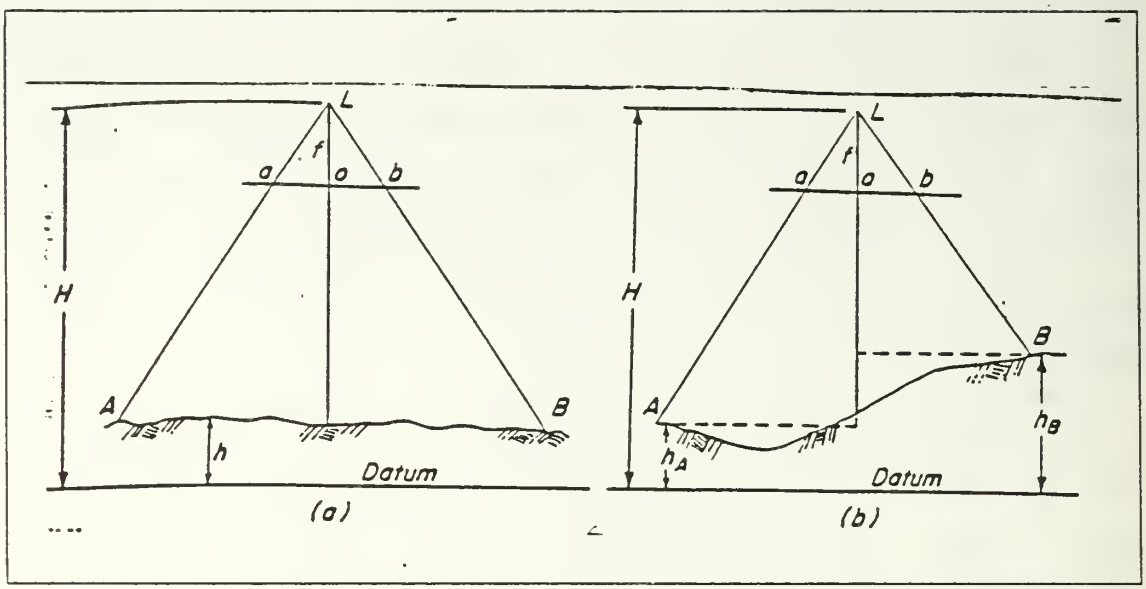

Figure 2.1 Scale Variation

The flight height H is ordinarily controllable by the pilot to within 1 percent (Slama,1980). Therefore, as can be seen from Figure 2.1 a, if the photograph is vertical, and if there is little variation in ground elevation, there is only a small variation in scales of the photographs obtained in any given flight. Thus in Figure 2.1 b the scales for the points A and B are given by the equations

$$S_A = f/(H-h_A) \qquad (2.2)$$

$$S_B = f/(H-h_B) \qquad (2.3)$$

where h_A and h_B are the ground elevations of the points A and B respectively. Specifications for aerial photographs

frequently require that if variations in scale exceed 5 percent, the photographs be rejected which was a criteria used in this study. Scale variation can be controlled somewhat by selecting appropriate flight/focal length combination.

The scale of an aerial photograph can also be obtained by comparing known distances utilizing the equation

$$S = ab/AB \qquad (2.4)$$

where ab is the measured film distance between images of two points on the ground which are at the same elevation or where the difference in elevation is small, and AB is the distance measured on the ground (see Figure 2.1).

A topographic map may be used to compute photographic scales. This is not recommended since undefined map errors are then propagated into all the work done with the photographs. The ground distances between two points can be computed by measuring the map distance between points which are well defined on photographs, and multiplying by the map scale. In turn, the photo scale can be determined by measuring the photo distance between the same points, and using Equation 2.4 to calculate the average photo scale for one photograph; several scales for the same photograph must be computed for different ground points. A large-scale (relative to the photo scale) map must be used to avoid measurement errors. The accuracy of this method will depend on the accuracy of the topographic map.

A very accurate method for determining the scale of photographs is to utilize ground control points. The accuracy of this method requires the existence of ground control points in the study area, good recovery of the existing ground control points, and images of ground control points that can be well identified on the photographs.

Ground control data are obtained using accurate surveying techniques. Ground control point identification is a most important step in photogrammetric mapping. Once the ground control data have been obtained, the photographic scale can be determined as follows:

a. The photo distances between the control points are determined by measuring the photo coordinates of the images of the ground control points.

b. Photographic scales are calculated utilizing Equation 2.4 each time for each pair of control points.

c. The average photographic scale is taken as the average of these scales. By emloying an average photographic scale, errors caused by tilt may be reduced.

If the scale of a photograph is unknown, it can be determined by making use of other photographs with known scales. This method requires the existence of photographs with known scales which cover the same area as the photograph with an unknown scale and images of points well identified in both photographs.

The procedure for scale determination includes the following steps:

a. The distance between two images is measured on the photo with the known scale.

b. The ground distance AB between the two points is calculated using Equation 2.4

c. The distance between the same images is measured on the photo with the unknown scale.

d. The scale of the photograph having the unknown scale is calculated from the Equation 2.4

e. Steps a. thru d. are repeated several times for different image points to calculate the average scale of the photograph and improve accuracy.

The accuracy of the computed photographic scale following the above procedure is not as high as for the

other methods mentioned previously because accuracy depends on the known scale of the photograph and elimination of other displacements.

2. Errors Due to Relief Displacement

As mentioned above, errors in measurements can be caused by elevation or relief differences. Because the ground is not usually flat, a photograph differs from a map. It is obvious from Equation 2.1 that the scales of the photographic images vary in accordance with the elevations of the corresponding objects on the ground, while the scale of a map is the same over the covered ground. Several methods for determining the average scale of a photograph were presented in the previous section. For a given method, the errors in the scale variation over the photograph can be reduced.

Ground relief also affects the displacement of the images on a photograph. This displacement is known as relief displacement and is defined as the displacement of images radially inward or outward with respect to the photographic nadir, depending on whether the ground objects are below or above the datum (Slama, 1980).

The nature of relief displacement is demonstrated in Figure 2.2 . The ground points A and B are above the datum and their photographic images a and b have been displaced radially outward from the center of the photograph. If the ground points A and B were at the datum elevation, their images would appear at a' and b'. Relief displacement is zero at the center (o) of the photograph. By using the simple geometry of Figure 2.3, relief displacement can be determined from the following equations:

$$d = r-r' = rh/H \qquad (2.5)$$

$$d = r'h/(H-h) \qquad (2.6)$$

where d is the relief displacement of the point, r is the radial distance on the photograph from the center to the image of the top of the object, r' is the corresponding distance from the base of the object, H is the flight altitude, and h is the elevation of the object.

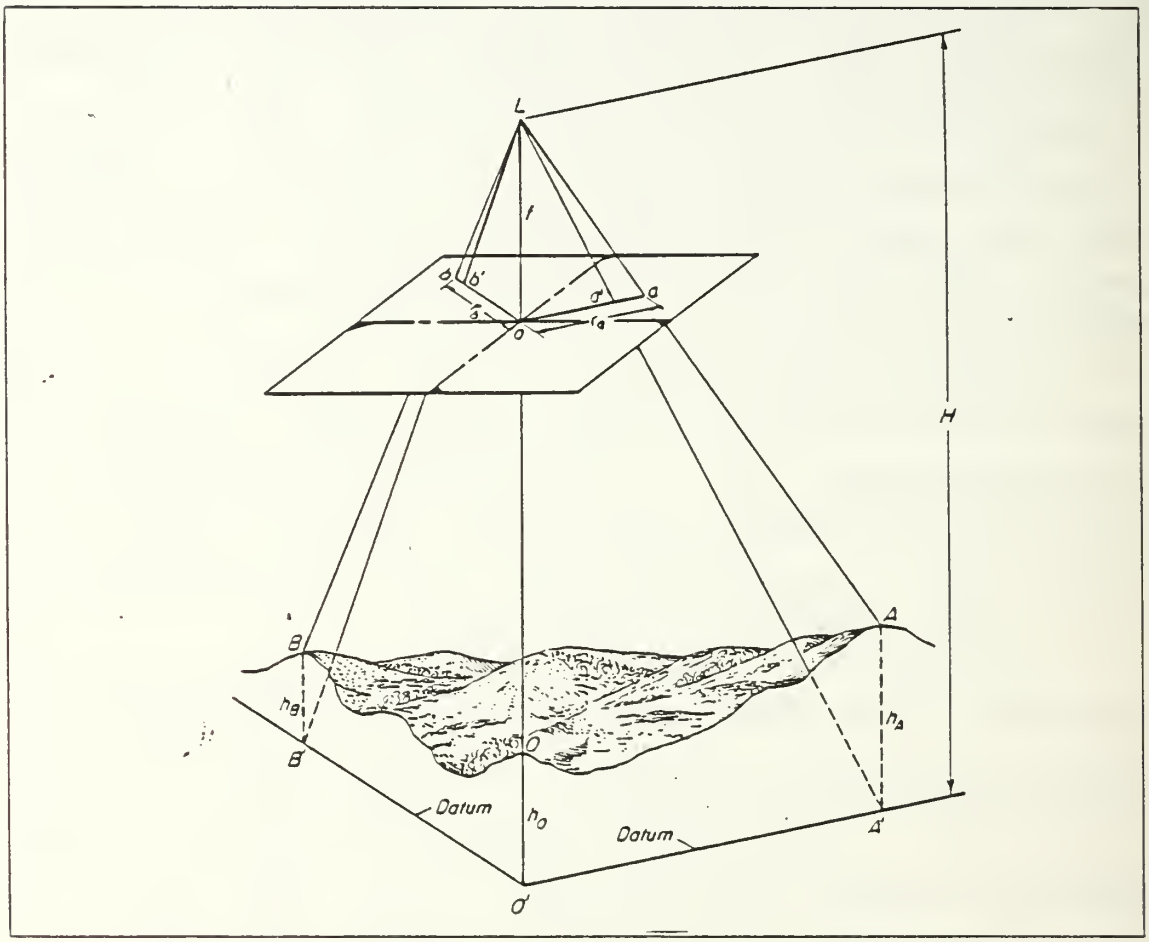

Figure 2.2 Relief Displacement on a Vertical Photograph

Equations 2.5 and 2.6, indicate that the magnitude of the displacement of an image is directly proportional to the elevation, h, of the object above or below the datum and

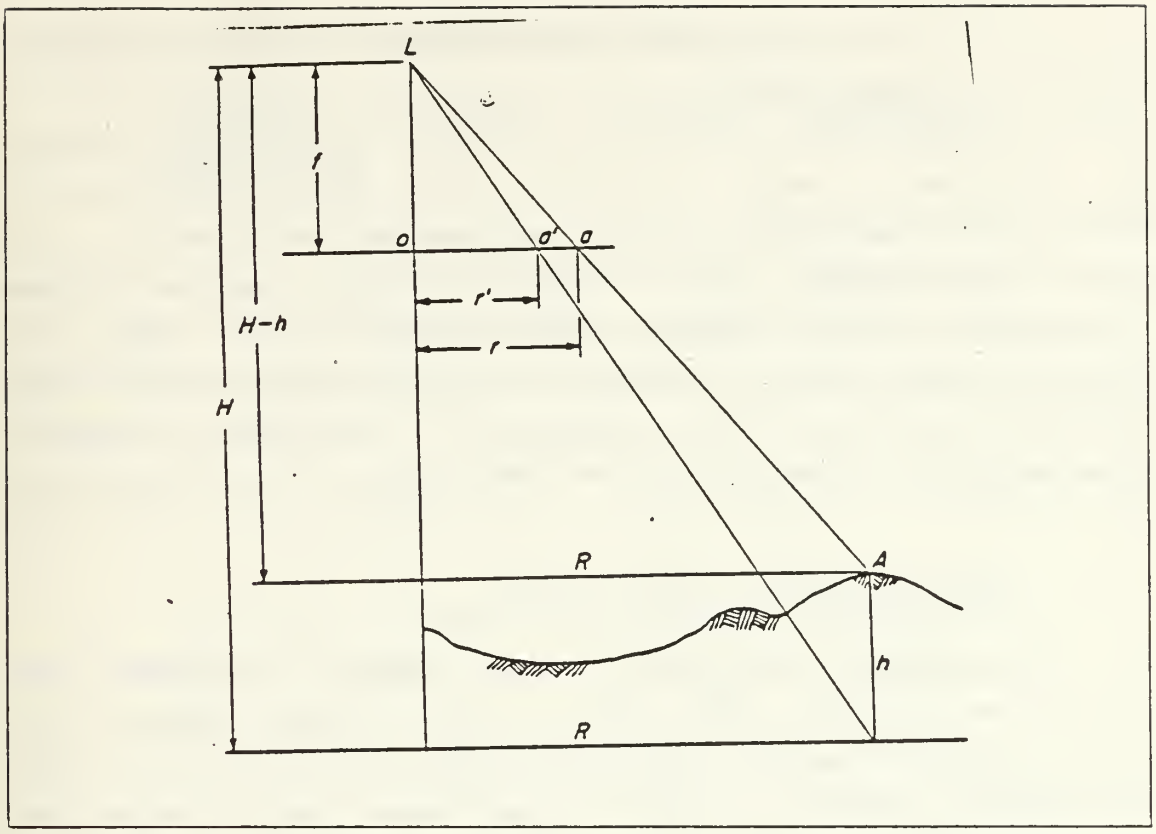

Figure 2.3 Relief Displacement of a Point

to the radial distance r or r' from the center of the image of the top or the base of the object respectively.

Errors due to relief displacement can be reduced by the following methods:

a. By choosing measurement points that have small differences in elevation from the average elevation of the terrain.

b. By choosing measurement points that are as near to the center of the photograph as possible; and

c. By computing the relief displacement of each measurement point and correcting the photographic coordinates of this point for the amount of the relief displacement.

d. By making the measurements on a stereo model rather on a single photo.

To calculate the value of the relief displacement, the elevation of each measurement point should be found as well as the flight altitude, H, and the radial distance, r, of the photographic image. The above terms may be applied to Equation 2.5 to find the displacement of the image. If the displacement, d, is known, the photographic coordinates of the point can be corrected. Additional details concerning this method will be examined in the following section.

3. Scale Variation Due to Tilt

Although photographs for mapping purposes are supposed to be taken vertically, often a small angular tilt of the aircraft occurs. The tilt angle is usually less than two degrees (Moffitt, 1980). The exact scale of a tilted photograph depends on the camera focal length, f , airplane altitude, H, above datum and the amount of the tilt. Methods exist to eliminate scale variations due to tilt, but require special instruments. Scale variation due to tilt is not eliminated in the present study. All photographs were assumed first to be truly vertical. If during the measurements the scale variation for a stereo model exceeds five percent, then the model is rejected. Five percent scale variation gives an error in the measurements of 0.15 ft (0.045 m) for each 3 ft (0.91 m) of ground distance. Additional details about tilted photographs are discussed in Appendix A.

C. DESCRIPTION OF RESEARCH PROCEDURE

1. Procedure to Select, Locate and Purchase Aerial Photographs

The first step was to select a location for study in order to select the aerial photographs. Several requirements were used to select the most suitable aerial photographs. These requirements were: resolution, height of the flight, sharpness, accuracy, and maximum scale. Once a photograph was selected, the next step was to locate the needed photogrammetric information, i.e., focal length, flying height, etc.

The areas studied were the shoreline and adjacent cliff between Monterey Harbor (36° 36' 05"N x 121° 53' 04"W) and Fort Ord's Stilwell Hall (36° 40' 00"N x 121° 49' 06"W), four specific locations were chosen for the study. The chosen areas were significant, because the success of the study of coastal erosion was contingent upon the avialability of suitable aerial photography.

To select the proper aerial photographs an approximate idea of the rate of erosion to measure was needed. Several studies of the region (Moffitt, 1968; Thompson, 1981) indicated average rates of erosion of 3.4 ft/yr (1.04 m/yr). On the basis of these it was established that photographic resolution for erosion measurements in a period of one year should be at least 3 ft (0.91m).

Another important factor was horizontal "resolution", the ability to separate adjacent features so that they can been seen as individual images and expressed as the maximum number of lines/mm that can be resolved. The standard emulsions used in photogrammetry yield a final image resolution of 40 lines/mm or more. When copies are made from original exposures, each copy of the image can degrade the resolution by about 15 to 20 percent. This

indicates that the resolution would be 36 lines/mm or more for the first copy. For the purpose of this study copies were used because the owners of the aerial photographs would not allow work with the originals. Therefore, the 36-lines/mm resolution allowed the use of copies of aerial photographs to scales of 1:36000 (Keller, 1975). Sharpness of imagery was a prime concern in the choice of the photographs. Films such as aerial Ektachrome provide more information to the viewer due to their higher spectral content. Black and white has been used for years with success, but resolution is limited by silver halide grain size.

Once criteria had been established for the selection of aerial photographs, an attempt was made to obtain existing photography, and to choose photographs best suited for a coastal erosion survey. Various government agencies that maintain permanent records of local aerial photographs were contacted. Sources most important in this respect are: U.S. Army Corps of Engineers; National Cartographic Information Center (NCIC); and the University of California at Santa Cruz.

NCIC has the most extensive records to be found. It has a system which is called the Aerial Photography Summary Record System (APSRS), this system offers a simple method to determine not only whether aerial coverage is available over a particular geographic location, but who was responsable for the photographic project, and the photographic parameters, i.e. the focal length, photographic scale, and film emulsion, etc., associated with each particular roll of film. A single set of aerial photographs for 1966 was purchased from NCIC.

The U.S. Army Corps of Engineers, San Francisco, indicated that they had sets of aerial photographs from 1946. We had copies of these printed at the U.S. Geological Survey (USGS), Palo Alto. The Corps of Engineers offices

in Los Angeles sent a set of copied aerial photographs for 1984; that flight was made expressly for the purpose of studying coastal erosion.

The Library of the University of California, Santa Cruz, has significant holdings of aerial photographs of Santa Cruz and adjacent areas; these include aerial photographs for the years 1956, 1976,1978 and 1981. The photographs are available as paper prints and are easy to locate by means of an index.

For future studies of the area, all the photographs we collected are available as strips that cover the entire shoreline from Monterey harbor to Fort Ord. Photographs purchased from NCIC, were printed with particular attention paid to enhancing the cliff tops. The size of the photographs used was 9" x 9"; only three sets were available in color, while the remaining three sets were in black and white.

2. Selection and Description of Subject Areas

The locations of the four areas chosen for study are indicated in Figure 2.4 . The general criteria for choosing the study areas were that a cliff be adjacent to the shoreline, the location be close to a development which had been affected by erosion, and that the area had been studied previously so that earlier findings could be compared with the proposed model. The distribution of the chosen areas gives a clear representation of the erosion rates between Monterey Harbor and to just north of Fort Ord.

The area adjacent to the Naval Postgraduate School's Beach Laboratory is approximately 1800 ft (549 m) long, and the average cliff elevation is approximately 19 ft (5.8 m) above Mean Lower Low Water (MLLW) The developments that bounded the area are the Monterey Regional Water Pollution Control Agency building to the north and the Del Monte Beach

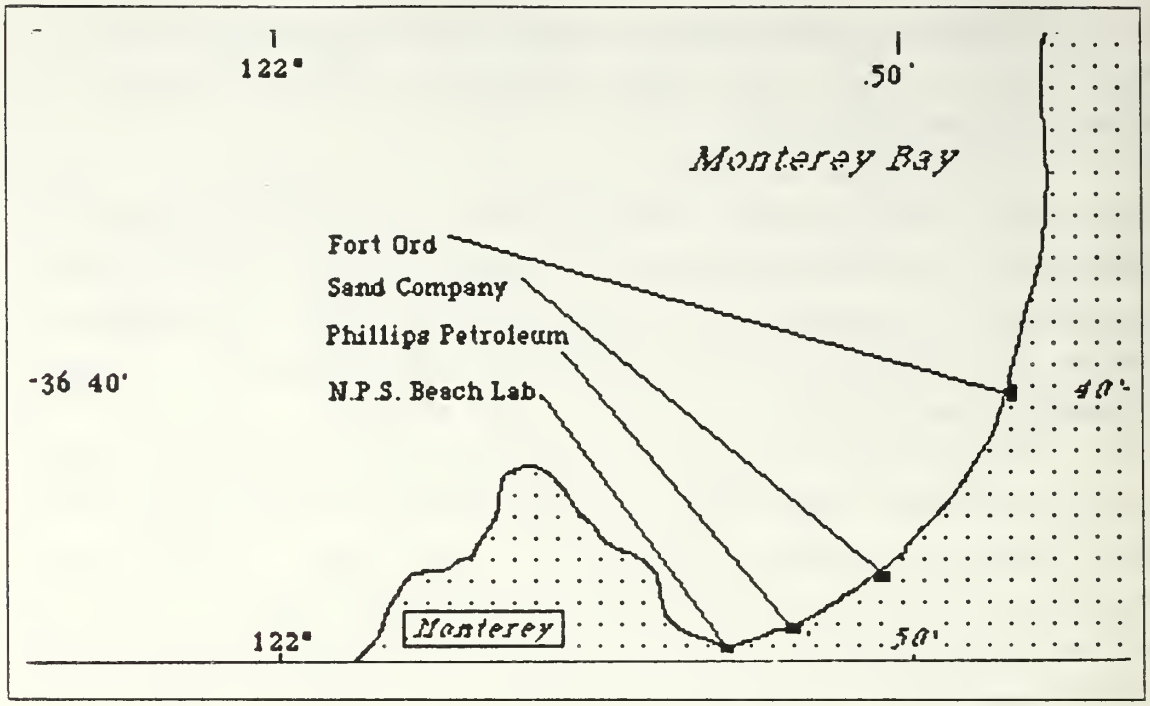

Figure 2.4 Selected Areas of Study

Town Houses to the south. No erosion studies had been previously conducted in this area, although the geographic situation was ideal for the study.

The waterfront of the Phillips Petroleum Property is approximately 660 ft (201 m) long, and the average cliff elevation is approximatelly 24 ft (7.4 m) above MLLW. The development that bounds the northern edge of the area is the Holiday Inn, where a vertical concrete wall was built to provide protection, and the development that bounds the southern edge is the Ocean House Apartments, where a granite rock revetment wall was constructed for erosion protection in 1983. Studies conducted by Thompson (1981) indicate an erosion rate here of 1.8 ft/yr (0.54 m/yr) between 1939 and 1978.

The waterfront of the Monterey Sand Company in Sand City is approximately 2200 ft (671 m) long and does not have

a development close by. However, it is possible that this sand mine contributes to the erosion of the southern area of the Monterey Bay (Moffitt, 1968).

The Fort Ord waterfront in our area of interest is approximately 3280 ft (1000 m) long, and the average cliff elevation is approximately 52 ft (15.85 m) above MLLW. Stilwell Hall is located at the center of this area and is in danger due to the erosion of the adjacent cliff. Smith (1983) summarized the erosion here as 6-7 ft/yr.

3. Selection of Reference Points

After selecting the four study areas, the next step was to choose stable points to reference the location of the shoreline. To achieve the greatest accuracy, special attention was given to the selection of reference points. Objects with sharp, well defined images on the photographs were selected as close as possible to the area being studied to minimize errors due to scale variation or tilt. The height of the reference object is not a problem, because the error due to relief displacement can be corrected. For example, in the area corresponding to the Beach Lab (NPS), street corners between Second Street and Sloat Avenue were choosen as reference points. The distances between these points were surveyed in the field to determine the scale of the photo.

The geometrical distribution of the reference point is important, because to compare identical areas for different years, it is necessary to specifically match geometrical figures.

4. Selection of Measurement Points

Several measurement points along the beach profile, such as high tide line, toe of the cliff, and top of the cliff, were considered (see Figure 2.5). Past measurements

indicate the beaches of southern Monterey Bay are eroding. Therefore, it was desired to choose a point that would be

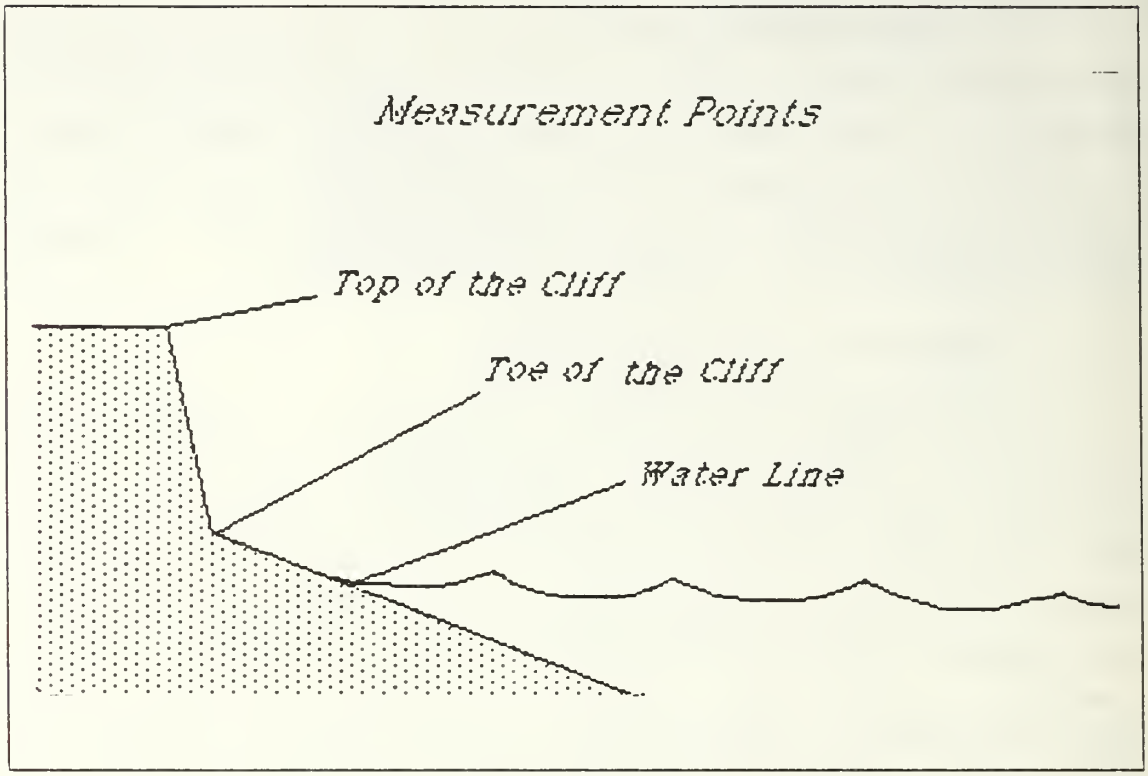

Figure 2.5 Selected Measurement Points

sharply defined in the aerial photograph and indicative of permanent change (erosion).

The beach profile at mean waterline is highly variable. Variability other than that due to erosion may be caused by: (1) Sea level changes due to tides (approximately 12-hour periods); (2) Sea level changes due to atmospheric conditions (hours to days variation); and (3) Seasonal variations in beach profile due to onshore-offshore sand transport. Similarly, variations at the high waterline may be caused by these factors. The bottom of the cliff can be affected by factors (2) and (3). Another factor which

can affect the measurements is slumping of cliff material, causing displacement of the base of the cliff .

The change in the location of the top of the cliff is a measure of permanent erosion; seventy per cent of the coast of Southern Monterey Bay is adjacent to cliffs having an average height of 30 ft. The erosion of cliff tops is due to slumping caused by erosion at the base of the cliff.

To use aerial photography several other factors must be considered which affect the accuracy of the measurement. In panchromatic black and white photographs the definition of the water line is not clear at scales smaller than 1/10000, and errors larger than 3 ft (1 m) are easy to make; wind surges have the effect of causing the high tide water level to be slightly higher or lower than the level due to tide alone, which causes some variations in horizontal locations of the high water line. A correction or adjustment of the high water line location to account for wind tides is not possible because of the lack of local wind data. In several black and white aerial photographs the bottoms of the cliffs were not clearly defined due to the shadow of the cliff. Even if the bottom of the cliff could be measured in one year, another year could indicate an apparent shoreline change due to the collapse of the cliff wall.

The sharp representation of the top of the cliff in aerial photographs offers a clear and identifiable point of reference. Therefore, long-term erosion was inferred by measuring the locations of the cliff tops.

To draw the contour of the cliff, reference points were selected as near to the beach as possible. The horizontal choice of points along the cliff was based on the topography and profile of the cliff. For instance, where the cliff formed a straight line, only two points were necessary, but in those cases where the cliff showed a different form, a sufficient number of points were measured to define the shape.

5. Measurement Techniques

After all reference points and contours of the cliff had been selected on the two sets of aerial photographs being compared, the measurement process began. The X-Y coordinates of photographic image points were obtained using a stereo comparator (Carl Zeiss 1944, Model # 96180).

A comparator is an instrument having two linear scales accurately assembled perpendicular to one another. The coordinates are read by comparing these linear scales. Precision is improved by the use of verniers, or micrometers, and other devices for reading the scales, and magnifiers to enable better pointing at the photographic images; thus, the absolute coordinate of images on a photo may be read to 0.01 mm. Measurements can be made separately on each photo of a pair, but point transfer is much better if a pair of comparators are assembled so that the photographs may be viewed stereoscopically. The absolute coordinates (X,Y) of each point can be obtained directly from the equipment, and the difference in elevation between two points can be determined directly by measuring the difference of parallax between them.

The parallax of a point measured on a pair of overlapping vertical photographs is equal to the X-coordinate of the point measured on the left-hand, X_ℓ, photograph minus the X-coordinate of the point measured on the right-hand, X_r, photograph. In this definition, the X-axis passes through the principal point and is parallel with the flight line, and the Y-axis passes through the principal point and is perpendicular to the flight line. Then,

$$dp = X_\ell - X_r \qquad (2.7)$$

where dp is the parallax deference.

To find the difference in elevation using the parallax measurement, the following equation was utilized:

$$dh = (H\ dp)/(dp + b) \qquad (2.8)$$

where H is the flight height above datum, b is the distance between the principal points of the two photographs (air base), and dh is the height difference.

To set up the photographs on the comparator it was necessary to determine the principal point of each photograph. For this purpose, it was necessary to utilize an overlay and to draw over the overlay two lines connecting opposing fiducial marks in the photograph. The intersection of these lines is the nominal principal point. Once the principal point of the photograph was established, it was transferred visually to the conjugate point corresponding to that principal point in the other photograph. Each photograph then had two points, the principal point and the conjugate point. These two points in each photograph were connecting with a straight line to draw the air base . The air base was aligned with the X-axis of the equipment to eliminate Y parallax.

Measurements were made as follows:

a. The first step was to find the X- and Y-coordinates of the principal points, and using them in Equation 2.9 to find the length of the air base.

$$(D_{12})^2 = (X_{O_1} - X_{O_2})^2 + (Y_{O_1} - Y_{O_2})^2 \qquad (2.9)$$

where D_{12} is the distance between the principal points or air base (b), X_{O_1} , Y_{O_1} represent the coordinates of the principal point of the left photo. X_{O_2} , Y_{O_2} represent the coordinates of the principal point of the right photo.

b. In the second step, the X- and Y-coordinates and X-parallax of the reference points were determined; in each set of photographs four reference points, A,B,C, and D, were always established. The ground distances AB and CD were always known by physical measurement in the field; therefore, by calculating the distances ab and cd from the photographs the scale of the photographs could be determined using Equation 2.4 . The reference parallax of the photograph was always the parallax of the reference points.These points were always chosen at the same elevation; therefore, any parallax difference was due to tilt and not to relief displacement. Tilt errors were reduced by averaging the scales.

c. The third step was to measure X- and Y-coordinates and X-parallax of the photographic images of the ground reference points and the points along the shoreline. All of the data were recorded on a data sheet. The procedure is explained in Appendix B.

d. The fourth step was to input all recorded data into the computer program (Appendix B) to reduce all of the photographic coordinates to ground coordinates at scale 1:2000 and to correct coordinates for relief displacement.

e. The fifth step was to plot all reduced coordinates on a chart at a scale 1:2000. For each area we obtained one chart per photograph and then matched all together at the reference points. For instance, for the Beach Lab area the south corner of the intersection of 2nd Street and Sloat Street was used as the reference point.

f. The sixth step was to find the following parameters: the average rate of erosion, its standard deviation, and the average volume eroded using the average elevations. This calculation was performed by a computer program using linear interpolation.

D. APPLICATION AND ANALYSIS OF COASTAL EROSION DATA

1. Presentation of Data

The cliff top contours for years 1946, 1956, 1966, 1976, 1978, and 1984 are presented for the four beach sections. Shoreline recession and erosion rates are determined from the cliff top contours. The cliff top contours indicate variability in the recession rates. It is assumed that the average erosion rate for each area is more representative than the erosion rates at any one point of the study area. Recession rates along the shoreline are not uniform. By averaging the recession rates at many locations along the shoreline the random measurement errors are reduced. The average recession rates for each study area are computed from the rates of change at number of points along the shoreline and are presented in the following sections. The standard deviation is also calculated and provides a measure of the variability of the erosion rate over the measured shoreline. The average volumetric erosion rate is calculated by multiplying the average top recession and the average cliff elevation.

2. Fort Ord

Fort Ord area has been divided into two regions, North and South of Stilwell Hall (Figure 2.6). The erosion directly fronting Stilwell Hall has been retarded by construction of a revetment, and the results in this region are not representative of the typical erosion. Therefore, the middle region was not taken into account in the calculation of erosion rates.

The variations of the shorelines for the period 1946 - 1984 are illustrated in Figures 2.7 and 2.8 in which it can be seen that erosion north of Stilwell Hall is more intensive than to the south of it. This is because the

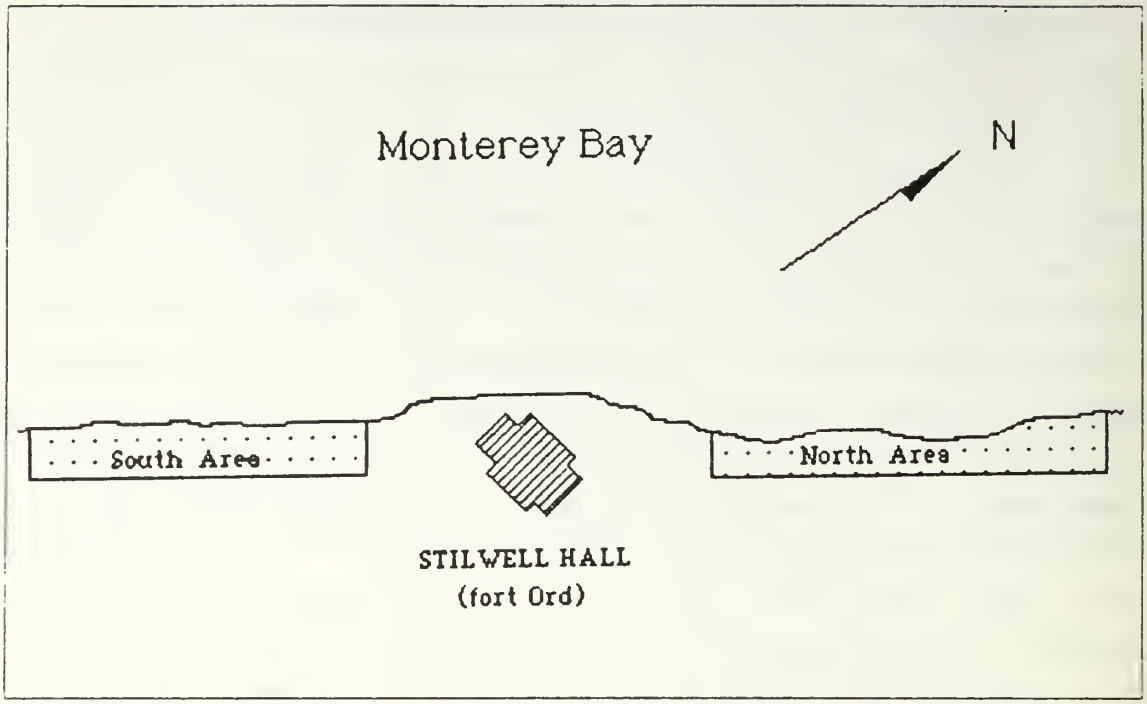

Figure 2.6 Fort Ord (Southern Monterey Bay)

beach to the south appears to be somewhat protected from storm waves from the north and west due to the presence of the Stilwell Hall revetment. The recession rates, standard deviations, and the average eroded volume are shown in Tables 1 and 2 . Data are shown for six time increments to give a record of change from 1946 until 1984, a total of 38 years. Of the five time intervals, the 1978-1984 interval had the most severe erosion for the North region, and the 1956-1966 interval for the Southern region. In the analysis of erosion during these intervals, the number and direction of storms is important. Storms during 1946-1984 period are listed in Appendix D.

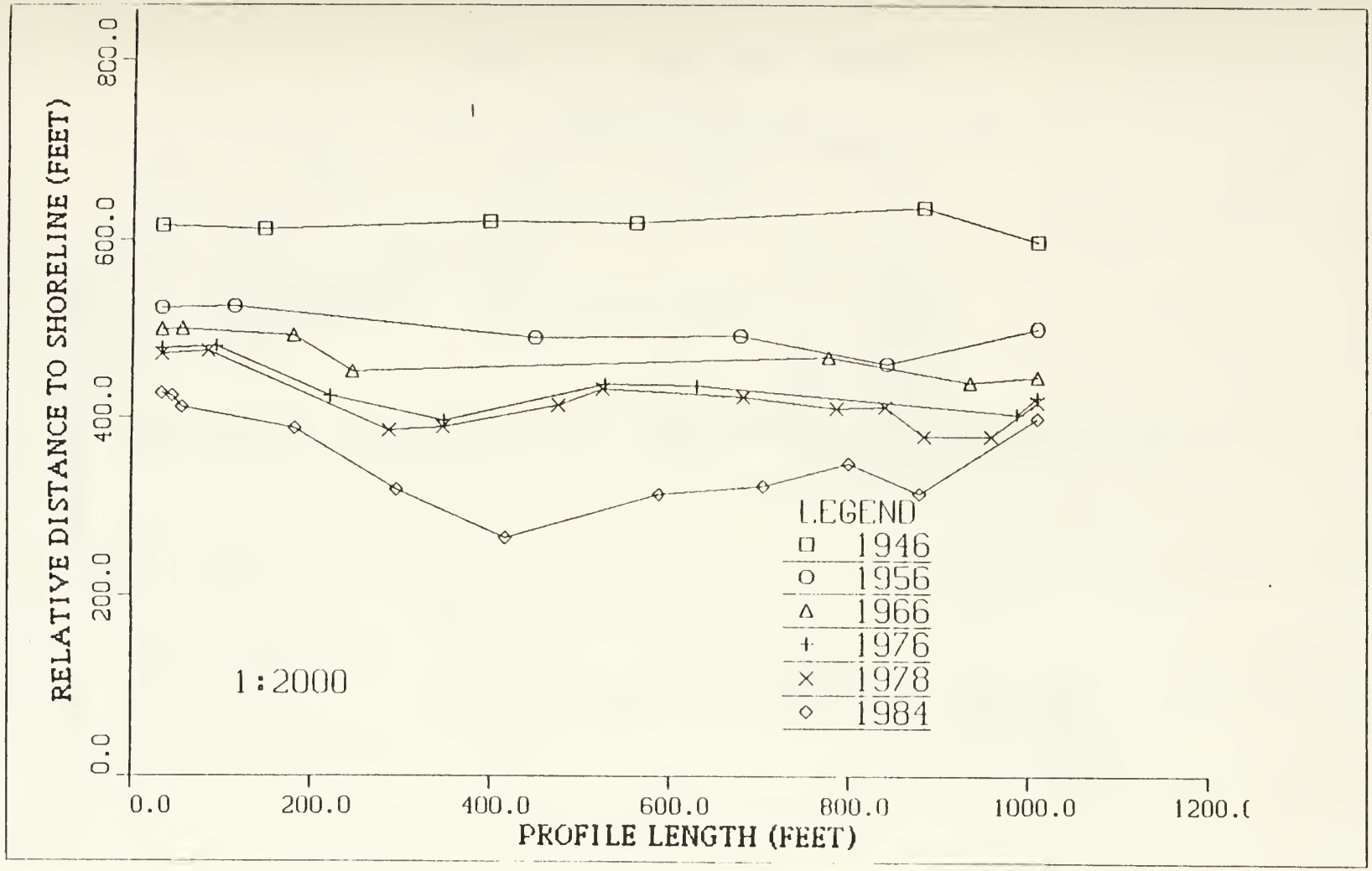

Figure 2.7 Fort Ord (North)

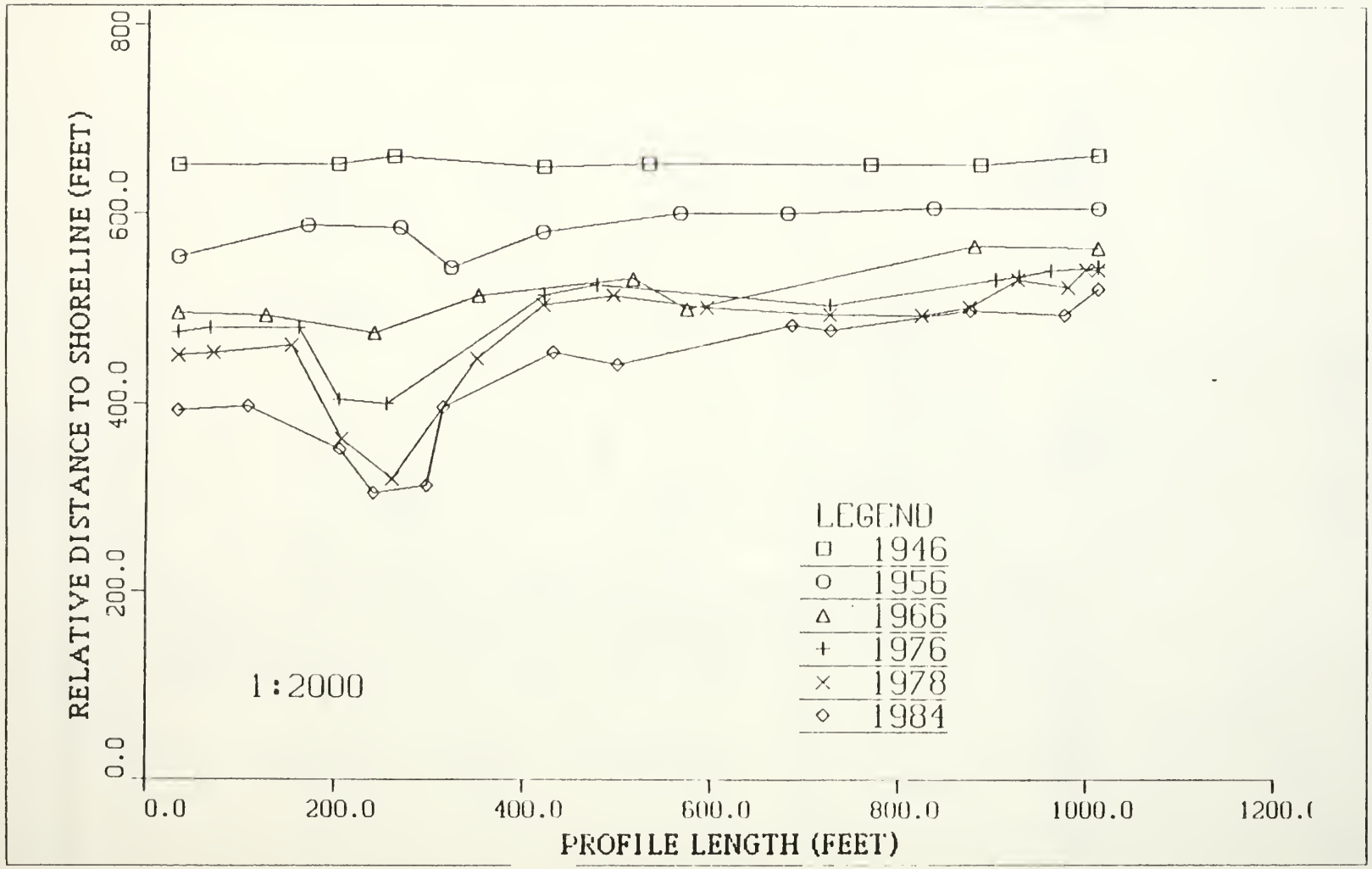

Figure 2.8 Fort Ord (South)

TABLE 1

Erosion Rate Results for Fort Ord (North Region)

LOCATION : Fort Ord North Area

AVERAGE CLIFF ELEVATION : 52 ft (above MLLW)

LENGTH : 1100 ft

TIME INTERVAL	RECESSION RATE ft/yr	STAND. DEV. ft	AVERAGE EROSION RATE $(ft^3/yr)/ft$
1946-1956	11.7	4.1	374.4
1956-1966	3.1	1.4	99.2
1966-1976	3.5	0.9	112.0
1976-1978	7.6	0.7	243.2
1978-1984	13.6	3.5	435.2
1946-1984	7.3		233.6

TABLE 2

Erosion Rate Results for Fort Ord (South Region)

LOCATION : Fort Ord South Area

AVERAGE CLIFF ELEVATION : 52 ft (above MLLW)

LENGTH : 1150 ft

TIME INTERVAL	RECESSION RATE ft/yr	STAND. DEV. ft	AVERAGE EROSION RATE (ft³/yr)/ft
1946-1956	6.5	1.7	208.0
1956-1966	6.9	2.1	220.8
1966-1976	2.5	2.3	80.0
1976-1978	4.8	1.7	153.6
1978-1984	6.0	2.2	192.0
1946-1984	5.7		182.4

3. Sand Dune

The Sand Dune region is shown in Figure 2.9 . The variations of the shoreline are illustrated in Figures 2.10 and 2.11 . The recession rates, standard deviations, and the average eroded volumes are shown in Tables 3 and 4 . The most severe erosion period is between 1976-1978 (8.8 ft/yr or 2.7 m/yr) for the southern region and between 1946-1966 (9.2 ft/yr or 2.8 m/yr) for the northern region. The annual rate of erosion during the measured period (1946-1984) is 6.3 ft/yr (1.93 m/yr) for southern region and 6.4 ft/yr (1.96 m/yr) for northern region, which are essentially the same rates.

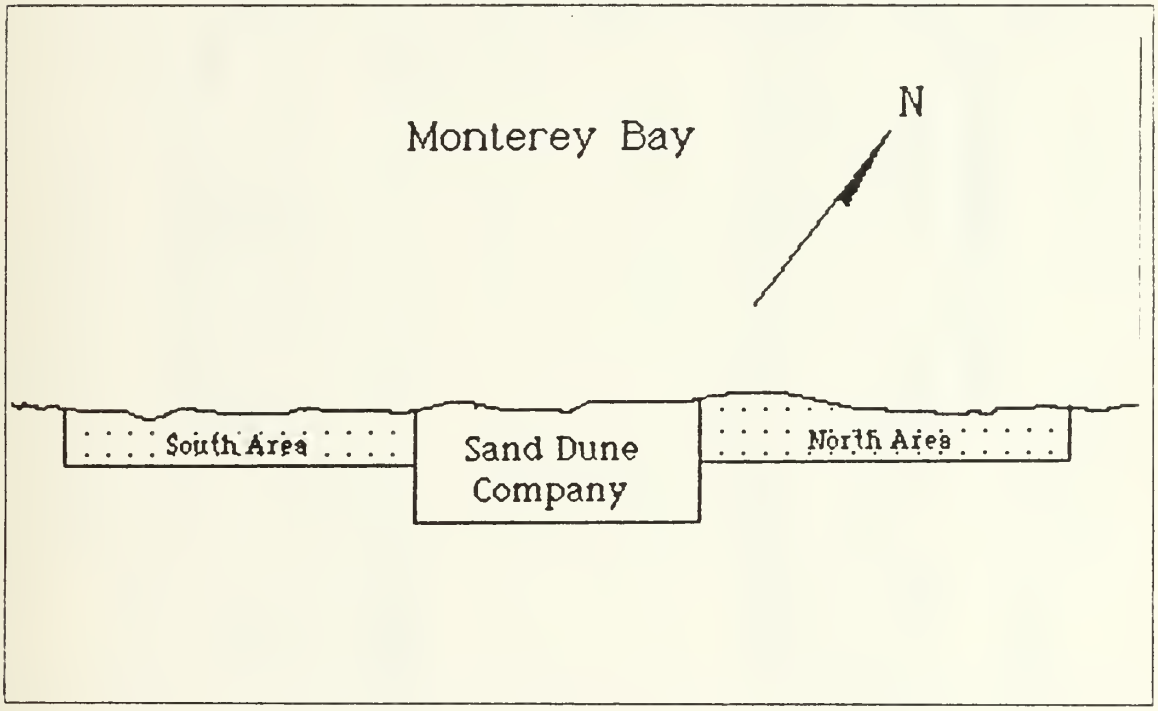

Figure 2.9 Sand Dune (Southern Monterey Bay)

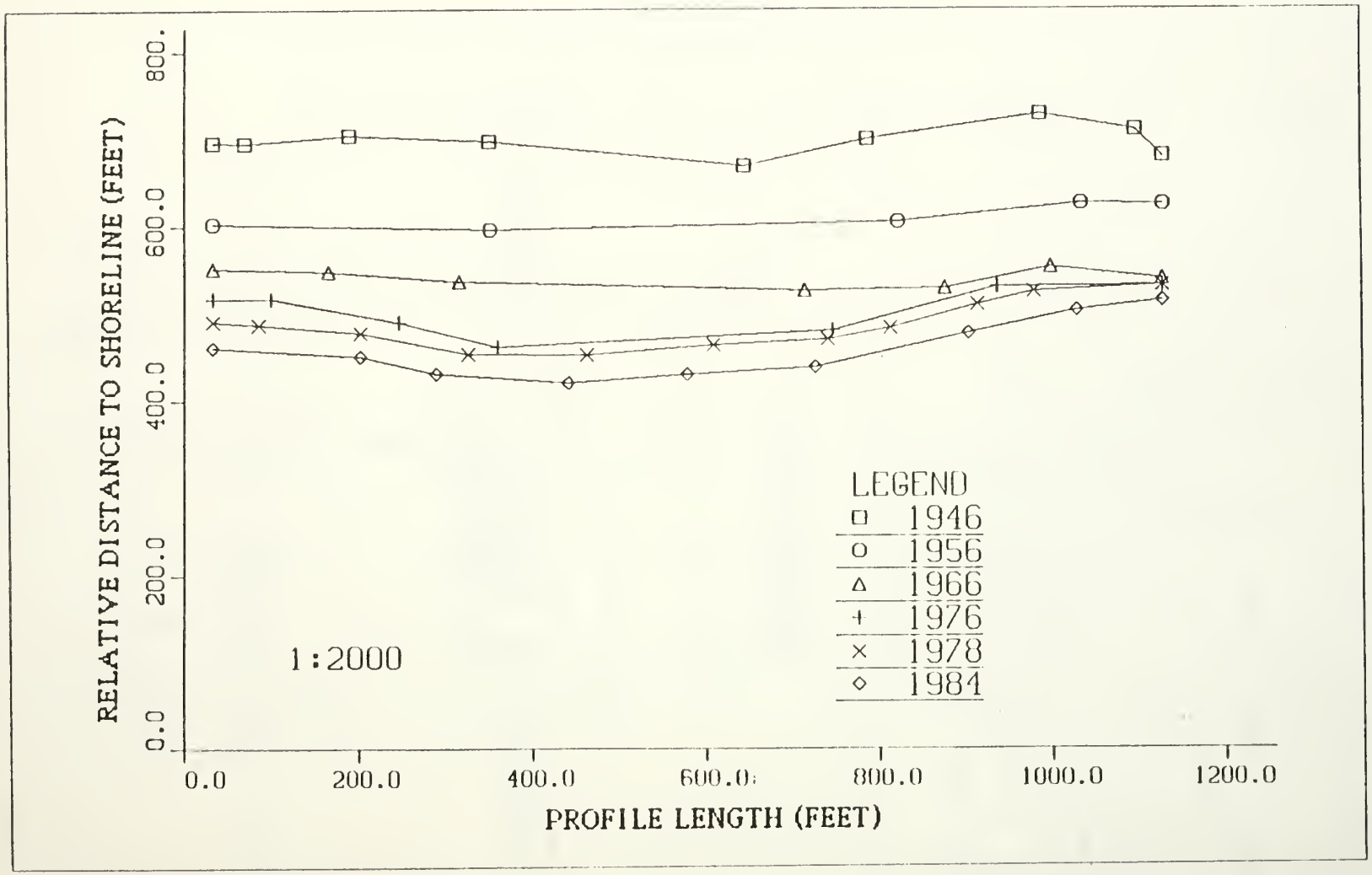

Figure 2.10 Sand Dune (North)

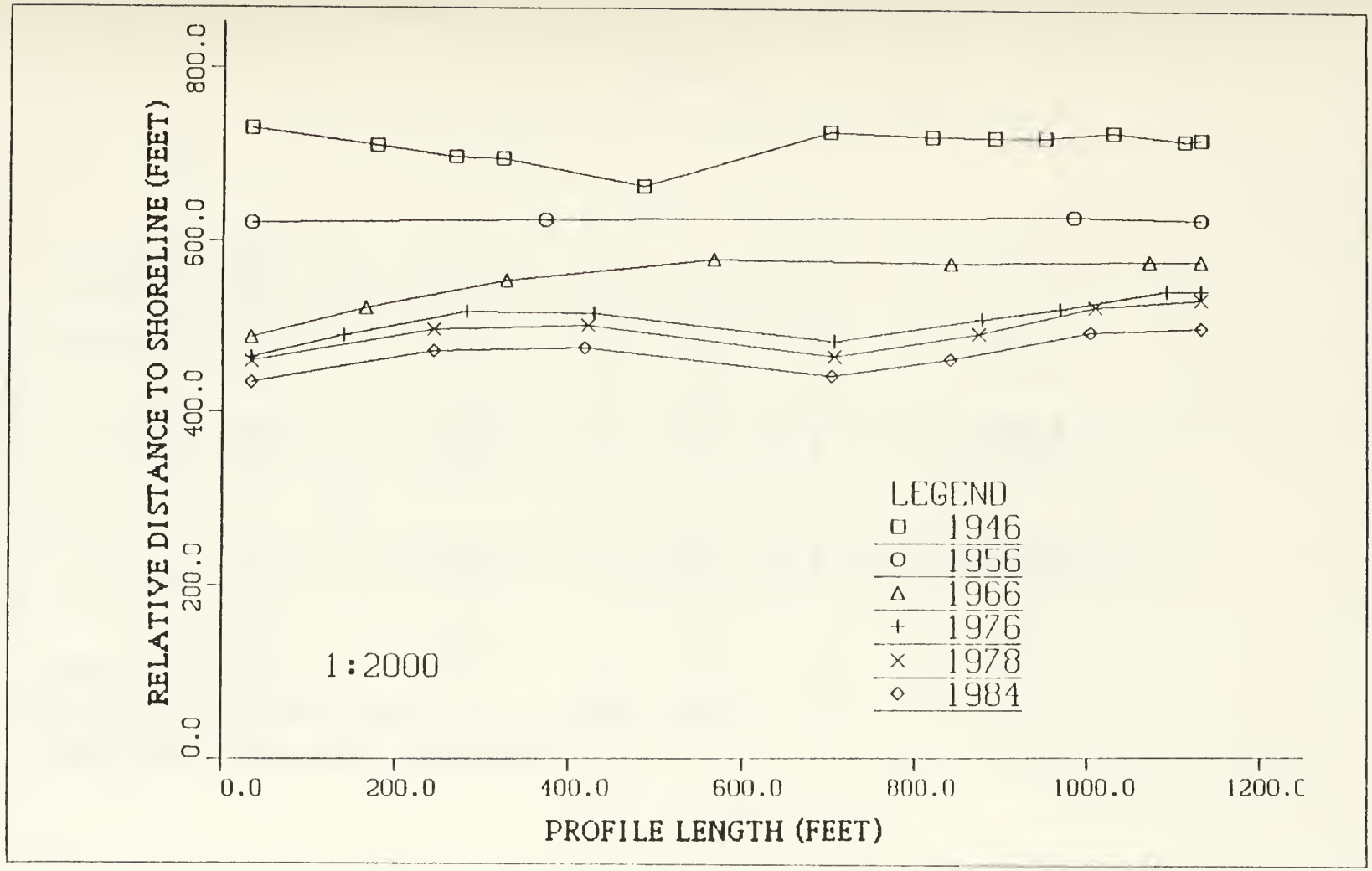

Figure 2.11 Sand Dune (South)

TABLE 3

Erosion Rate Results for Sand Dune (North Region)

LOCATION : Sand Dune North Area

AVERAGE CLIFF ELEVATION :29 ft (above MLLW)

LENGTH : 1100 ft

TIME INTERVAL	RECESSION RATE ft/yr	STAND. DEV. ft	AVERAGE EROSION RATE $(ft^3/yr)/ft$
1946-1956	9.2	1.2	147.2
1956-1966	6.8	1.0	108.8
1966-1976	4.1	1.9	65.6
1976-1978	8.9	0.7	142.4
1978-1984	4.8	0.3	76.8
1946-1984	6.4		102.4

TABLE 4

Erosion Rate Results for Sand Dune (South Region)

LOCATION : Sand Dune South Area

AVERAGE CLIFF ELEVATION : 27 ft (above MLLW)

LENGTH : 1150 ft

TIME INTERVAL	RECESSION RATE ft/yr	STAND. DEV. ft	AVERAGE EROSION RATE (ft/yr)/ft
1946-1956	8.2	1.8	123.0
1956-1966	6.6	2.2	99.0
1966-1976	5.2	2.2	78.0
1976-1978	8.8	0.4	132.0
1978-1984	4.3	0.2	64.5
1946-1984	6.3		94.5

4.. Phillips Petroleum Property

The Phillips Petroleum property is shown in Figure 2.12 . Erosion in the southern part of this region is more intensive than in the northern part (Figure 2.13). The recession rates, standard deviations, and the average eroded volumes are shown in the Table 5 . The most severe erosion is seen to have occurred in the 1976-1978 interval.

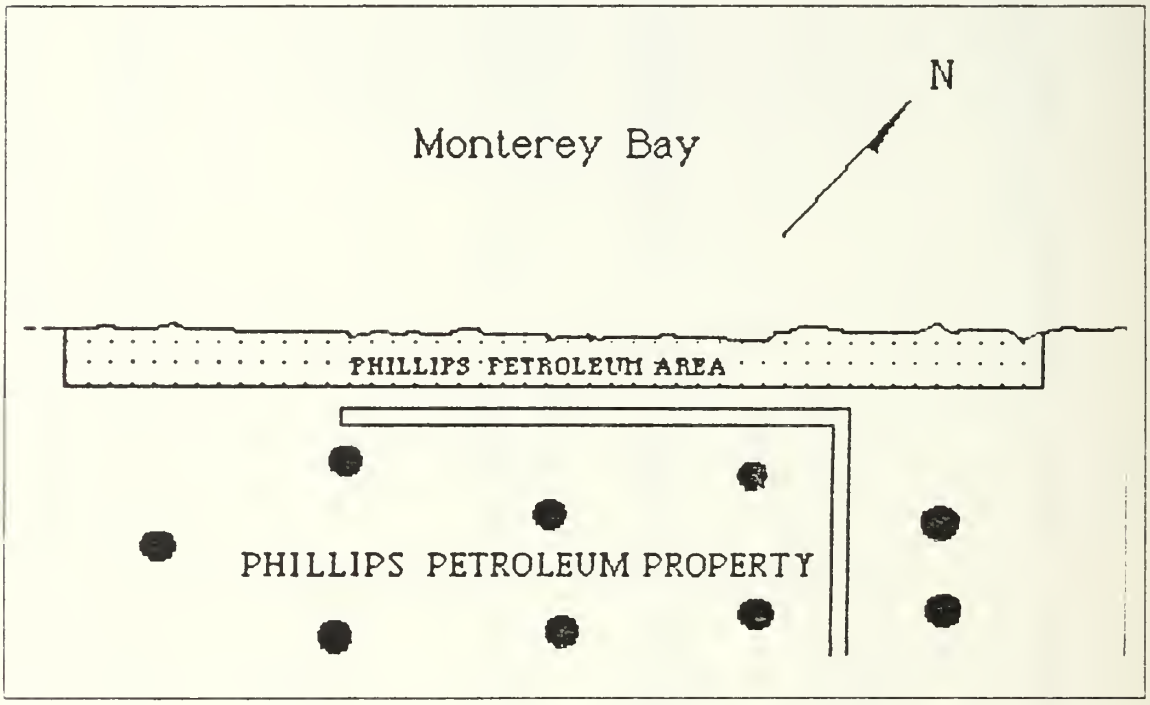

Figure 2.12 Phillips Petroleum Property

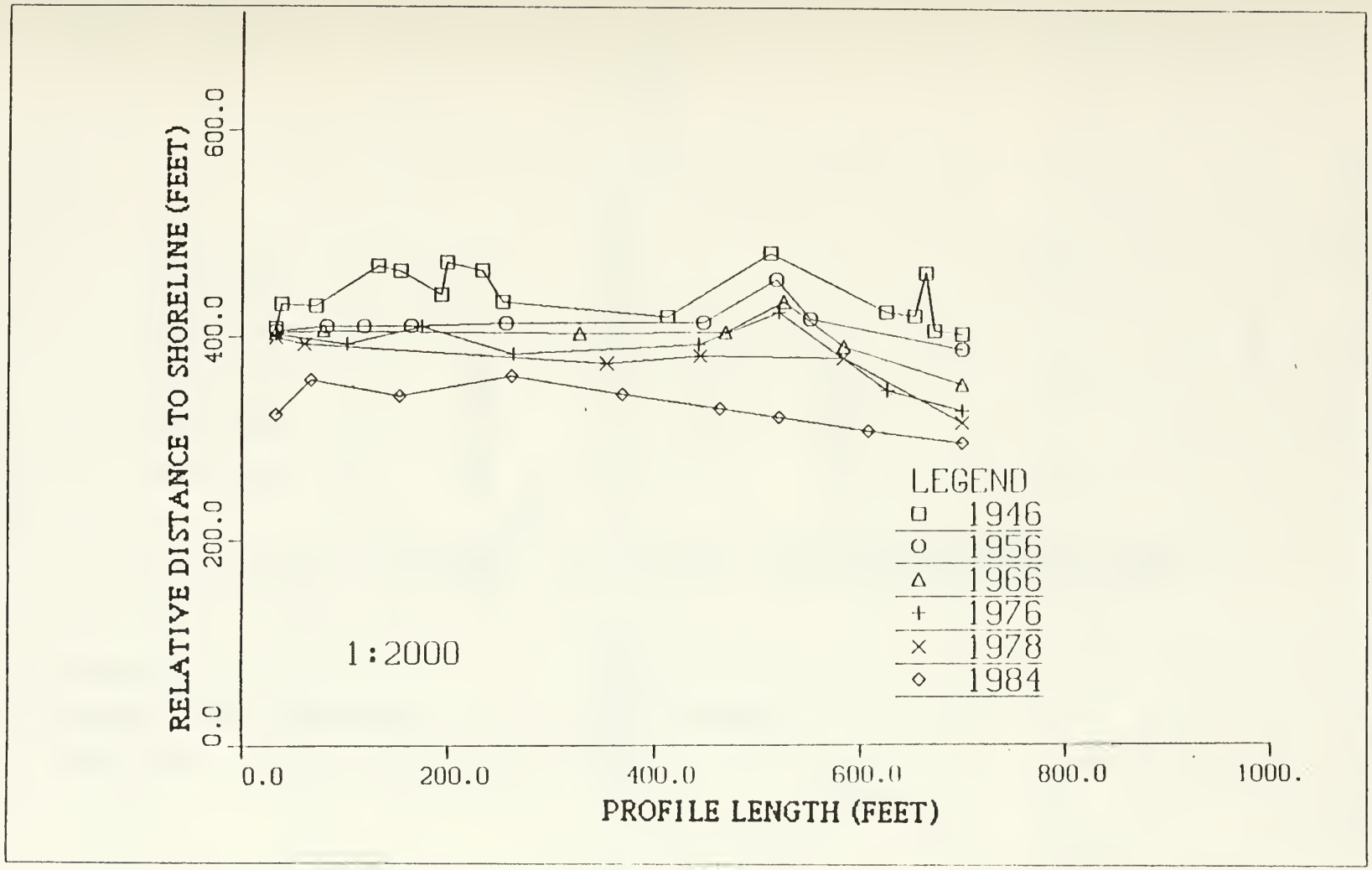

Figure 2.13 Phillips Petroleum Property

TABLE 5

Erosion Rate Results for Phillips Petroleum Property

LOCATION : Phillips Petroleum area

AVERAGE CLIFF ELEVATION : 24 ft (above MLLW)

LENGTH : 660 ft

TIME INTERVAL	RECESSION RATE ft/yr	STAND. DEV. ft	AVERAGE EROSION RATE (ft/yr)/ft
1946-1956	2.9	1.4	31.9
1956-1966	1.3	0.9	14.3
1966-1976	1.3	0.8	14.3
1976-1978	7.2	1.0	79.2
1978-1984	6.7	1.4	73.7
1946-1984	2.8		30.8

5. Beach Lab

The Beach Lab region is shown in Figure 2.14 . The variations of the shorelines are illustrated in Figures 2.15 and 2.16 . The recession rates, standard deviations, and average eroded volumes are shown in Tables 6 and 7 . The highest rate of erosion occured during the 1976-1978 interval, both at the northern end (4.2 ft/yr or 1.3 m/yr) and at the southern end (3.1 ft/yr or 0.95 m/yr). The average annual recession rate between 1946 and 1984 is 1.9 ft/yr (0.59 m/yr) for the northern and the southern region.

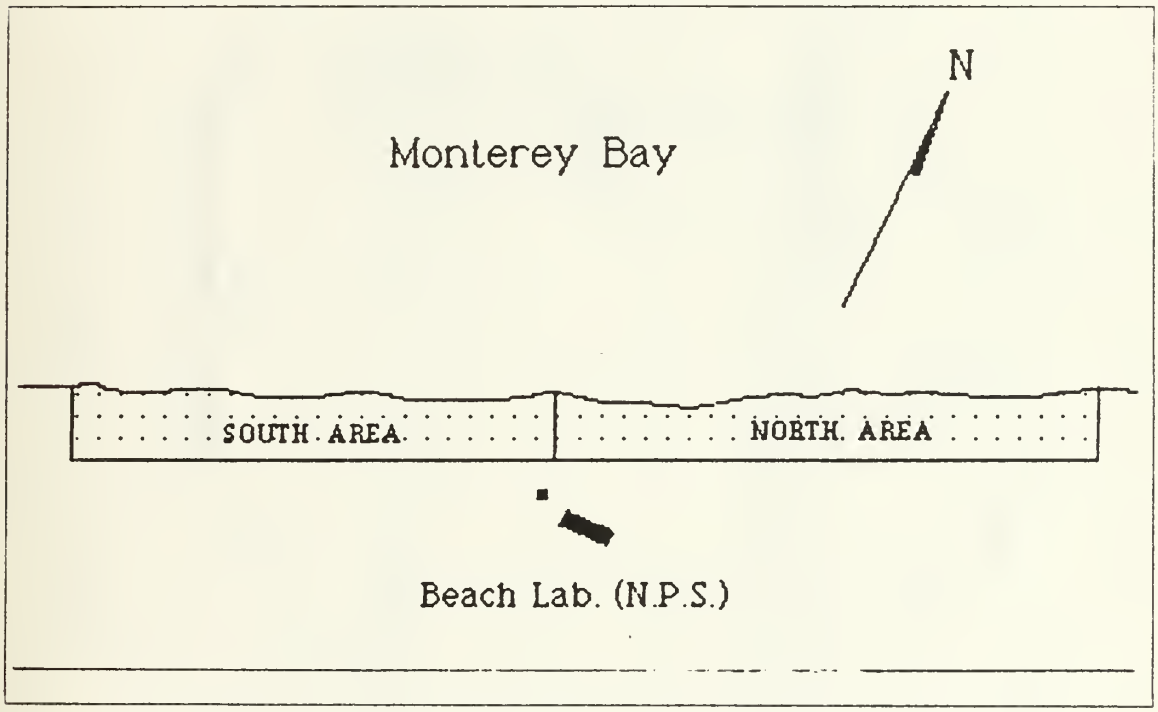

Figure 2.14 Beach Lab (Southern Monterey Bay)

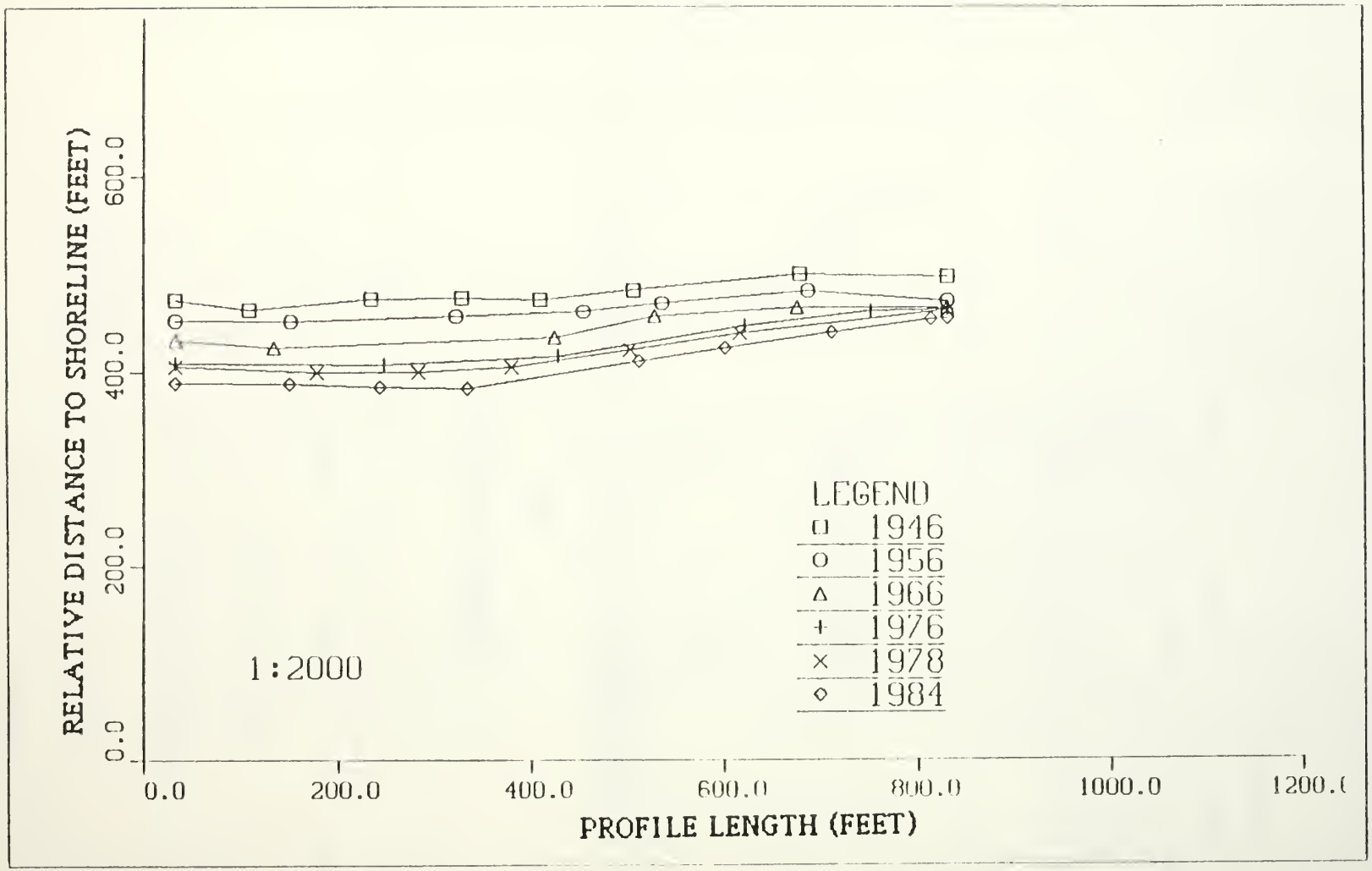

Figure 2.15 Beach Lab (North)

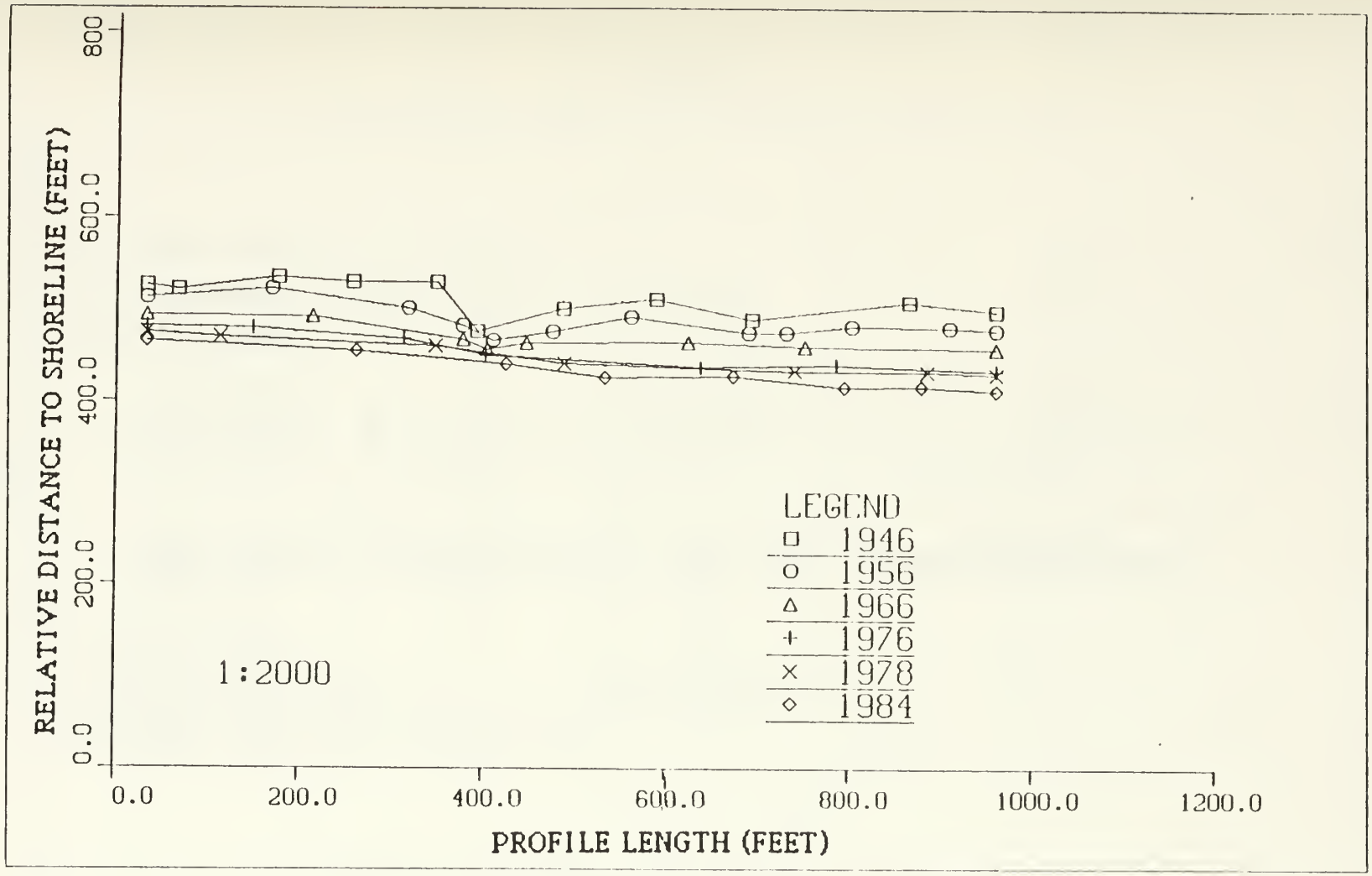

Figure 2.16 Beach Lab (South)

TABLE 6

Erosion Rate Results for Beach Lab (North Area)

LOCATION : Beach Lab North Area

AVERAGE CLIFF ELEVATION : 22 ft (above MLLW)

LENGTH : 850 ft

TIME INTERVAL	RECESSION RATE ft/yr	STAND. DEV. ft	AVERAGE EROSION RATE $(ft^3/yr)/ft$
1946-1956	1.8	0.3	18.0
1956-1966	1.9	0.6	19.0
1966-1976	1.6	0.7	16.0
1976-1978	4.2	0.2	42.0
1978-1984	2.2	0.3	22.0
1946-1984	1.9		19.0

TABLE 7

Erosion Rate Results for Beach Lab (South Area)

LOCATION : Beach Lab South Area

AVERAGE CLIFF ELEVATION :16 ft (above MLLW)

LENGTH : 1050 ft

TIME INTERVAL	RECESSION RATE ft/yr	STAND. DEV. ft	AVERAGE EROSION RATE $(ft^3/yr)/ft$
1946-1956	1.8	0.6	7.2
1956-1966	2.1	0.5	8.4
1966-1976	1.7	0.5	6.8
1976-1978	3.1	0.3	12.4
1978-1984	1.9	0.3	7.6
1946-1984	1.9		7.6

6. Comparison with Earlier Studies and Comments

The results of this and previous erosion studies are summarized in Figure 2.17 for Southern Monterey Bay. The average erosion rate is a minimum in the southern part and increases northward, with a maximum average erosion rate of 7.3 ft/yr (2.2 m/yr) at the northern Fort Ord region. No significant discrepancies were found between the results of the present study and those of earlier studies. For the southern part of the Beach Lab region Jones (1983) found the recession rate to be 1.1 ft/yr (0.33 m/yr). The difference between recession rates of the present study and Jones' is +0.8 ft/yr (0.24 m/yr). The recession of the cliff toe at the Phillips Property was previously studied by Thompson (1981); he found a recession rate of 1.8 ft/yr (0.54 m/yr), while we found 2.8 ft/yr. An earlier study of the Sand Dune region was performed by Moffitt (1968), who observed a recession rate of 6.9 ft/yr (2.1 m/yr). The difference between the erosion rate he found and ours is 0.6 ft/yr (0.18 m/yr). The Fort Ord region was studied previously by Jones (1983). The erosion rates he found do not appear to be consistent with ours, but they do show - as we do - that the northern part is eroded more rapidly than the southern part.

With only a few exceptions the cliff tops always recessed shoreward between photographs. This is contrary to the findings of earlier investigators (Thompson, Moffitt, Jones). The earlier studies indicate in some time intervals, accretion occurred along sections of the shoreline. This is not surprising, because they measured the position of the toe of the cliff or of the waterline, which we have shown to be unreliable. Thompson measured the toe of the cliff, which would indicate accretion in the case when the cliff slumps down. He did not remove errors caused by

relief displacement and he did not use an accurate photogrammetric instrument (mirror stereoscope) for his measurements. Moffitt measured the variation of the shoreline using as reference the position of the waterline. He corrected the location of the waterline for the tidal fluctuation, but he did not take into consideration the seasonal variation and the meteorological effects in sea level variation. Jones measured some simple points (one to three points) for each region using a mirror stereoscope without removing the effect of the relief.

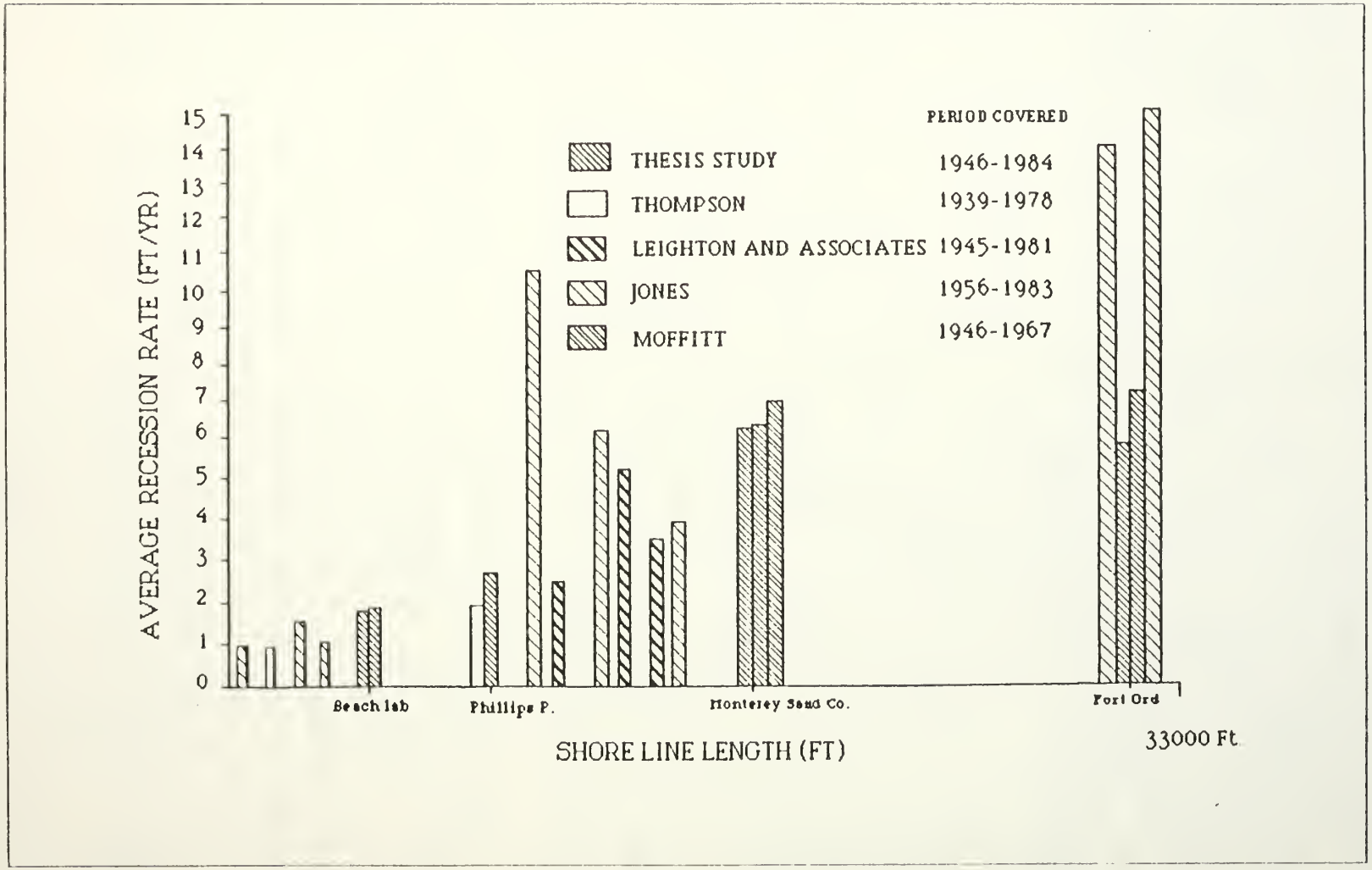

Figure 2.17 Average Recession Rates in Southern Monterey Bay

III. TIDES

The range of astronomical tides and sea level variations caused by oceanic and atmospheric factors must be taken into account when studying coastal processes. A major factor responsible for episodic erosion events is the simultaneous occurrence of high tides and storm waves. As the sea rises and falls with the tide, different elevations of the beach become subject to the action of the sea. On a tideless coast, the area of beach coming under any particular part of the wave action is small in dimension and is limited by the size of the waves themselves; the position of the break point remains essentially constant for constant wave height. On the other hand, if the tidal range is considerable, the break point of the waves moves in and out with the tides. The effect of swash can be exerted over a wide stretch of beach (King, 1959). The rise and fall of the sea due to tides is regular and predictable. Some additional, usually minor, short term factors that may influence the coastal sea level are: changes in atmospheric pressure over the ocean surface, changes in average density of the sea water column due to temperature and salinity changes, and wind set-up or set-down against the coast due to storms (Bretschneider, 1980).

An example of a combination of factors which can cause extreme sea levels occurred along the coast of California during the winter of 1982-1983. This winter, now commonly known as the " El Niño Winter ", was in many respects the most severe storm season in several decades along the Pasific Coast of North America (Quiroz, 1983). The extreme high tides were a result of warmer than normal mixed upper ocean temperatures associated with a strong 2-year El Niño

current, a storm surge due to low atmospheric pressure and persistent on-shore winds. On the average, the water temperature is coolest in spring, resulting in lower sea levels, and warmest in autumn, resulting in higher sea levels. Flick and Cayan (1984) studied the extreme sea levels which occurred in the San Diego area. They concluded that until about July, the observed sea level was close to normal, but by fall and early winter it exceeded the 1960-1978 average by up to 0.5 ft. This condition persisted through 1983. Sea level finally returned to near normal in December 1983.

Tides can be predicted by harmonic analysis using tidal constituents. Harmonic analysis of tides is based upon the assumption that the rise and fall of the tide at any locality can be expressed mathematically as the sum of a series of harmonic terms having certain relations to astronomical conditions. The general equation for the height, h, of the tide at any time, t, is given by

$$h = H_o + f_n H_n \cos(\sigma_n t - (k_n - (V_o + u)_n) \qquad (3.1)$$

where: Ho = mean value of the tidal observations; f = node factor of constituent; H_η= mean amplitude of the constituent in degrees per solar hour; k_η = epoch of the constituent at t=0 for period of observation; $(Vo + u)_\eta$ = value of argument of constituent at t=0 for period of observation; n = corresponds to particular constituent being computed (Schureman, 1971).

The Monterey tide station is located on Municipal Wharf No. 2 where the water depth is approximately 6.8 meters (Figure 1.1). Both a standard float-well tide gauge and a Fisher-Porter, bubbler type, Automatic Digital Recorder are used to record tidal data continuously on a strip chart and on punched tape, respectively. The records are sent to NOS for processing and analysis.

The Tidal Predictions Branch of NOS, Rockville, Maryland, performed a harmonic analysis of the observed tidal data for 13 years, isolating 37 harmonic constituents. These constituents are estimates of the periodicities and amplitudes of the components of the tidal force.The values of 20 constituents whose amplitudes were greater than 0.02 ft are used to predict the tides in the present study.

The data for each tidal constituent include: mean amplitude of the constituent H, local epoch of the constituent (Kappa), and the modified epoch of the constituent (Kappa prime). The data are listed in Appendix C. Additional information required for each constituent are the node factor, f, speed of the constituent, a, and the local value (Vo+u) which are found using Tables and formulas as follows:

a. Speed of the constituent, a, (Table 2 of Schureman, 1971)

b. Node factor, f, (Table 14 of Schureman, 1971)

c. Greenwich (Vo + u), (Table 15 of Schureman, 1971)

$$\text{Local}(Vo + u) = \text{Greenwich}(Vo + u) - (k' - k) \qquad (3.2)$$

The tides at Monterey are mixed, predominantly semi-diurnal, and are composed of two low and two high water levels per 24.8-hour tidal cycle. An example of the predicted tides is illustrated in Figure 3.1 .

Maixner (1973) and Bretschneider (1980) examined the differences between predicted and observed tides at Monterey. In their work, predicted heights were subtracted from hourly observed heights to yield non- astronomic residuals, or tidal anomalies. The differences have a frequency distribution which closely resembles a Gaussian distribution (Figure 3.2). Analysis of hourly sea level observations over the 13-year period of record show that 94.5% of the

observations lie within +/- 0.5 ft. of the predicted tide and 99.9% of the deviations lie within +/- 1.0 ft. Deviations of sea level from predicted values are the result of the complex interactions of atmospheric pressure, wind, variations in velocity of longshore currents and changes in average density of the water column (Bretschneider, 1980).

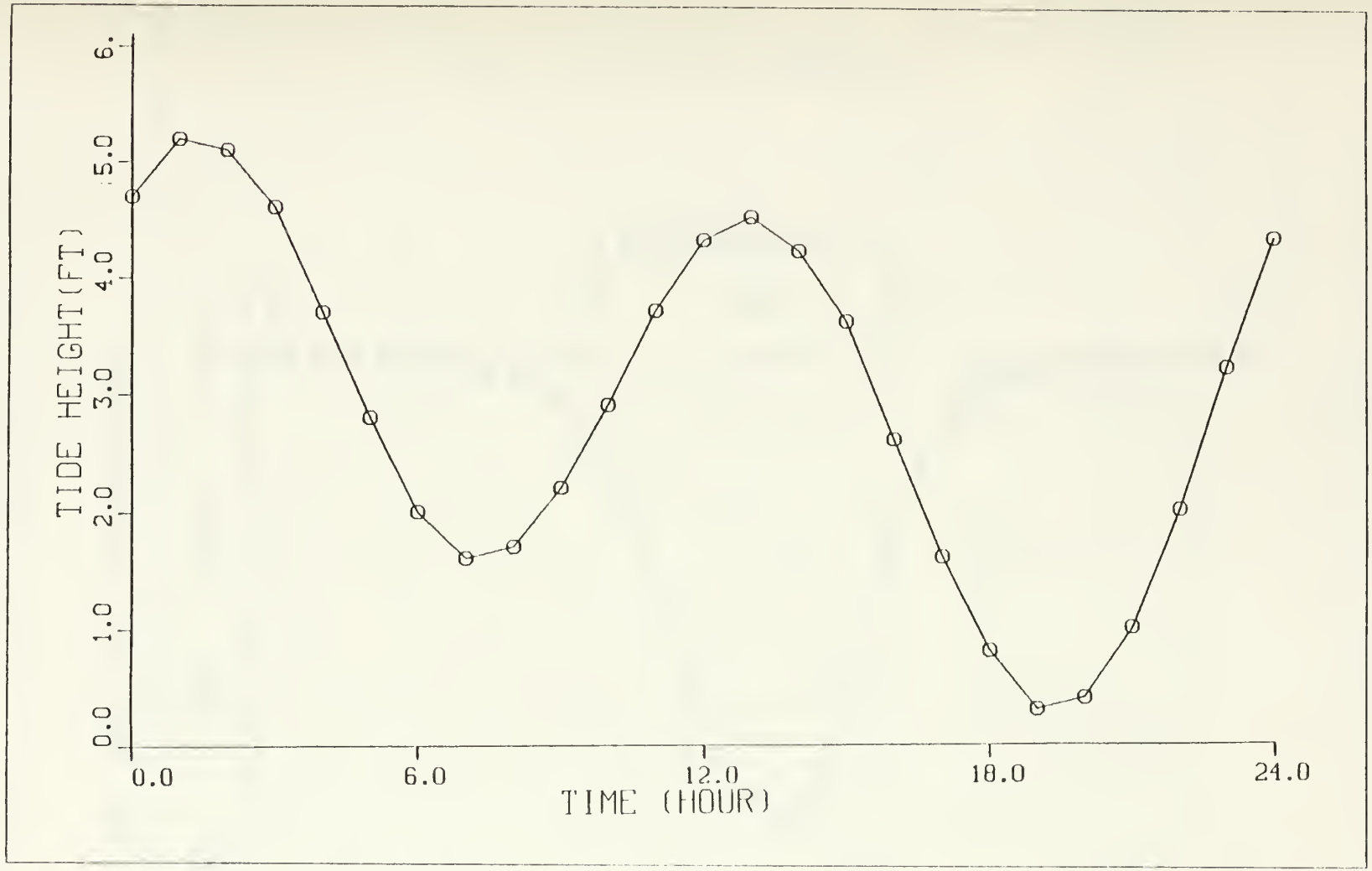

Figure 3.1 Typical Tidal Cycle for Monterey Bay

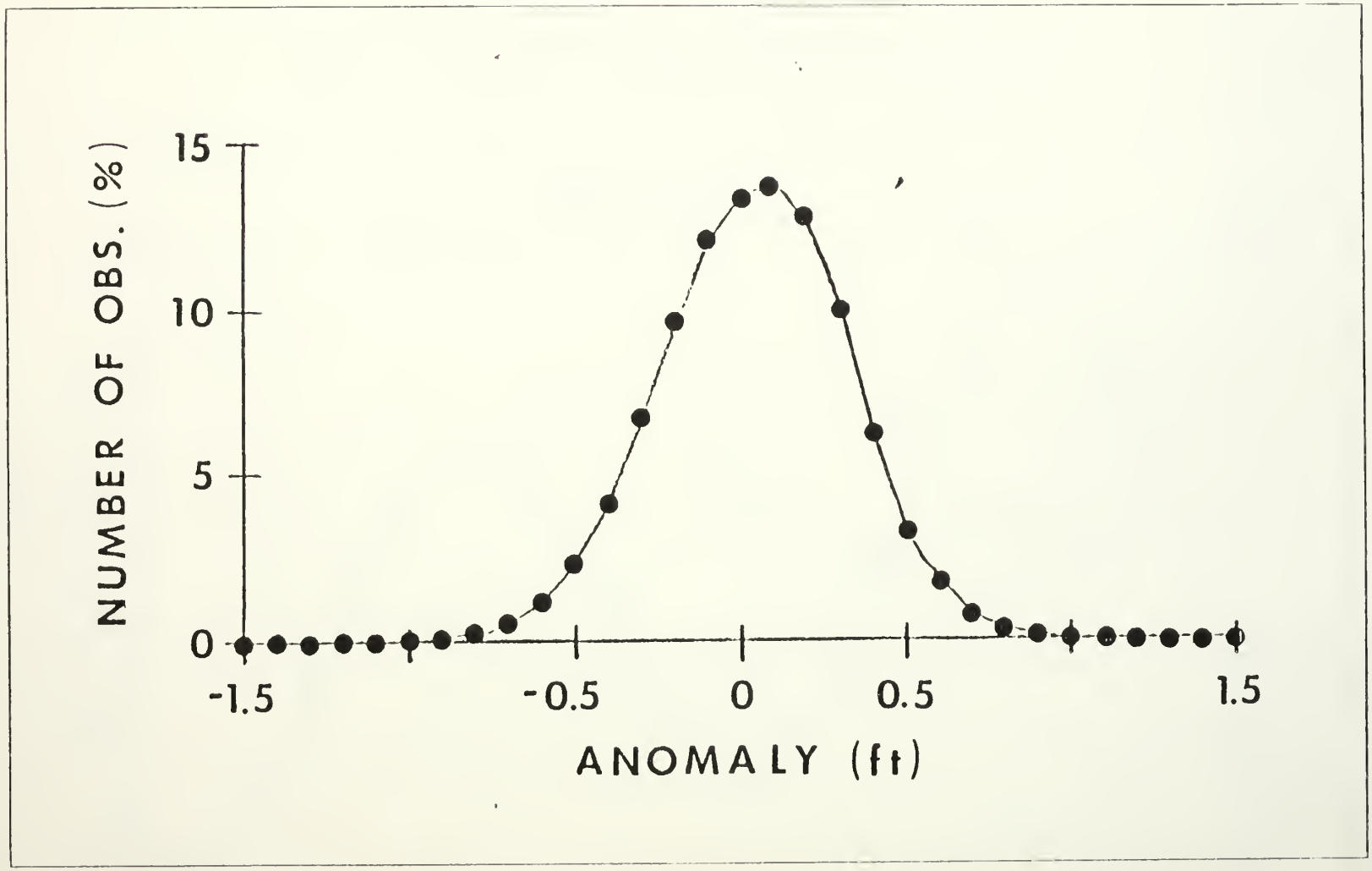

Figure 3.2 Tidal Anomalies

IV. SEA AND SWELL RUN-UP

A. WAVE CLIMATOLOGY

Wave action is the most important factor in the study of beach erosion. A wave climatology for Monterey Bay was calculated using deep water wave spectra obtained from Fleet Numerical Oceanography Center (FNOC). The deep water waves are transformed by refraction and shoaling into shallow water. The purpose of this study is to obtain wave characteristics in shallow water which are directly related to beach erosion.

The wave information is based on a 21-year (1964-85) climatology generated using the spectral ocean wave model (SOWM) for the entire North Pacific Ocean. SOWM is the present operational wave spectral model used daily by the Fleet Numerical Oceanography Center to predict waves in the Northern Hemisphere. The model has been operational since December 1974. Prior to this date a less accurate non spectral model was used. Because of the recognized importance of long-term wave statistics, it was decided to reanalyze the wind fields prior to 1974 and re-hindcast the waves using the spectral model to form the basis for a wave climatology. Thus, meteorological data on winds and weather over the Northern Hemisphere were reanalyzed and used to compute improved wind fields over the ocean. These improved wind calculations were, in turn, used to compute wave spectra for a grid of 1,575 points for every six hours for twenty years. For the period since December 1974 the "nowcasts" of the wave spectra based on observed winds every six hours have been saved for use in expanding the climatology.

The spectral ocean wave model can be described as being composed of wave generation, propagation of swell, and dissipation components. The growth of wave energy for a given wind velocity at grid points is accomplished by a modified Miles-Phillips technique. Growth is limited by the Pierson-Moskowitz fully-developed spectrum for a given wind speed. Directions are obtained through an equation derived by the Stereo Wave Observation Project. The wave energy spectrum at each grid point is represented by a 15-frequency by 12-direction matrix.

Energy for each frequency and direction is then propagated as dispersive swell into adjoining grid points. An Icosahedral-Gnomic map projection is used for the world's oceans, as the adjoining grid points form the correct great circle routes of swell propagation. The hindcasts are for the Northern Hemisphere oceans only and do not include swell that has propagated from the Southern Hemisphere.

Dissipation is included in the model to account for the effect of opposing winds and losses at high frequencies that occur as the swell propagates away from a generation area. The SOWM has been verified (Lazanoff and Stevenson, 1975; Pierson, 1982) and shown to give reasonable estimates of wave spectra (Thornton, 1983).

B. WAVE TRANSFORMATION FROM DEEP TO SHALLOW WATER

The waves are transformed by refraction and shoaling as they propagate from deep to shallow water. The wave velocity varies along the crest of a wave as the wave is moving at an angle to depth contours. This variation causes the wave crest to bend toward alignment with the contours. This bending of the wave is known as wave refraction. Refraction has significant influence on the wave height and distribution of wave energy along a coast. The changes of

wave direction of different parts of the wave results in convergence or divergence of wave energy. Refraction diagrams were calculated using a version of Dobson's (1967) linear refraction program. A topographic grid was generated using digital bathymetry provided by NOAA. The depths are the average of all historical measured depths in a 6 second grid given by Latitude and Longitude and referenced to mean-higher-high-water (MHHW). Since there were some grids without values, an interpolated, filled and smoothed bathymetry was generated using a DISSPLA subroutine. The mercator grid was then projected to a cartesian grid oriented north-south with a 200 meters grid spacing.

Assuming conservation of energy flux and long-crested waves, the wave variance density in shallow water (subscript h) is related to the deep water variance density (subscript o) by

$$S_h(f,\theta) = K_r^2(f,\theta)\, K_s^2(f)\, S_o(f,\theta_o)\, J \qquad (4.1)$$

$$\begin{bmatrix} 15 \\ X \\ 12 \end{bmatrix} = \begin{bmatrix} 15 \\ X \\ 12 \end{bmatrix} \begin{bmatrix} 1 \\ X \\ 12 \end{bmatrix} \begin{bmatrix} 15 \\ X \\ 12 \end{bmatrix} \qquad (4.2)$$

where f is the wave frequency; θ, the wave direction; Kr, the refraction transfer function; Ks, the shoaling transfer function and J, the Jacobian of the transformation. The matrix multiplication is indicated by Equation 4.2

The shoaling effects are due to a change in the group velocity, Cg, of the waves which to the first order is a function of depth and period. The shoaling transfer function is given by

$$k_s^2(f) = \frac{c_{g_o}(f)}{c_g(f)} \qquad (4.3)$$

Assuming energy density is conserved between wave rays, the refraction coefficient is given by

$$k_r^2(f,\theta) = \frac{b_o(f,\theta)}{b(f,\theta)} \qquad (4.4)$$

where b(subscript o) is the wave ray separation in deep water and b is the wave ray separation water having a depth of 4m.

Wave refraction diagrams were calculated for 5 directions in 30-degree increments from 185.5 to 335.5 azimuth and 12 periods (7.5 to 25.7 s). Examples of refraction diagrams for wave periods of 15 s and 25.7 s are shown in Figures 4.1 and 4.2 . The calculated refraction coefficients for each study area are shown in Tables 8, 9, 10, and 11 . Wave refraction studies show the four sites we studied to be protected from open ocean waves from the south and north, and only waves from the WNW to WSW can deliver significant energy. The study showed that, due to wave refraction, the open ocean waves impinge upon the shore within a narrow range of angles (Thornton, 1983). A value of Kr greater than one results in an amplification of wave energy whereas Kr less than one results in a decrease in energy. Examination of the refraction coefficient tables show that the coefficents are mostly less than one and in general are greater at Fort Ord and decrease to the south. Amplification does occur for some wave components from the west at Fort Ord; winter storms are often from the west. Amplification occurs for some wave components from the WNW (305.5) at Sand Dune and Phillips Property, but the components for other directions are significantly reduced due to refraction. No amplification of components occurs at the Beach Lab.

TABLE 8

Wave Refraction Coefficients (Ft. Ord Area)

Direction / Period (s)	305.5	275.5	245.5	215.5	185.5
7.5	0.88	0.95	0.43	0.36	0.16
8.57	0.86	0.94	0.44	0.46	0.18
9.73	0.85	0.93	0.52	0.42	0.18
10.91	0.81	0.92	0.49	0.47	0.18
12.4	0.74	0.95	0.60	0.72	0.17
13.85	0.80	0.99	0.49	0.49	0.17
15.00	0.57	1.02	0.47	0.60	0.15
16.40	0.77	1.20	0.48	0.52	0.18
18.00	0.62	0.92	0.52	0.44	0.19
20.00	0.47	1.17	0.55	0.38	0.15
22.5	0.37	1.28	0.80	0.32	0.19
25.7	0.47	0.44	0.70	0.38	0.17

TABLE 9

Wave Refraction Coefficients (Sand Dune Area)

Direction / Period (s)	305.5	275.5	245.5	215.5	185.5
7.5	0.83	0.33	0.22	0.21	0.10
8.57	0.82	0.33	0.24	0.29	0.13
9.73	0.80	0.33	0.24	0.44	0.16
10.91	0.78	0.31	0.34	0.31	0.14
12.4	0.77	0.32	0.28	0.49	0.13
13.85	0.81	0.43	0.26	0.32	0.17
15.00	0.74	0.51	0.32	0.39	0.14
16.40	0.72	0.44	0.31	0.33	0.13
18.00	0.72	0.37	0.32	0.38	0.18
20.00	1.37	0.36	0.27	0.19	0.14
22.5	0.84	0.33	0.23	0.25	0.12
25.7	1.02	0.39	0.25	0.27	0.10

TABLE 10

Wave Refraction Coefficients (Phillip Petroleum Area)

Direction / Period (s)	305.5	275.5	245.5	215.5	185.5
7.5	0.79	0.26	0.22	0.21	0.10
8.57	0.76	0.28	0.24	0.29	0.14
9.73	0.73	0.32	0.26	0.45	0.14
10.91	0.70	0.31	0.30	0.49	0.14
12.4	0.66	0.28	0.34	0.58	0.13
13.85	0.68	0.29	0.33	0.43	0.18
15.00	0.77	0.35	0.34	0.40	0.16
16.40	1.55	0.39	0.32	0.31	0.17
18.00	1.20	0.51	0.32	0.40	0.19
20.00	0.58	0.40	0.25	0.30	0.18
22.5	0.65	0.40	0.24	0.24	0.17
25.7	0.69	0.40	0.20	0.12	0.17

TABLE 11

Wave Refraction Coefficients (Beach Lab Area)

Direction / Period (s)	305.5	275.5	245.5	215.5	185.5
7.5	0.76	0.28	0.25	0.23	0.11
8.57	0.74	0.29	0.27	0.33	0.15
9.73	0.73	0.35	0.29	0.33	0.19
10.91	0.72	0.31	0.34	0.33	0.16
12.4	0.74	0.27	0.32	0.34	0.15
13.85	0.73	0.30	0.40	0.34	0.16
15.00	0.81	0.34	0.40	0.35	0.17
16.40	0.72	0.37	0.32	0.43	0.17
18.00	0.78	0.47	0.31	0.46	0.18
20.00	0.94	0.43	0.19	0.67	0.18
22.5	0.62	0.39	0.21	0.25	0.19
25.7	0.45	0.44	0.19	0.20	0.17

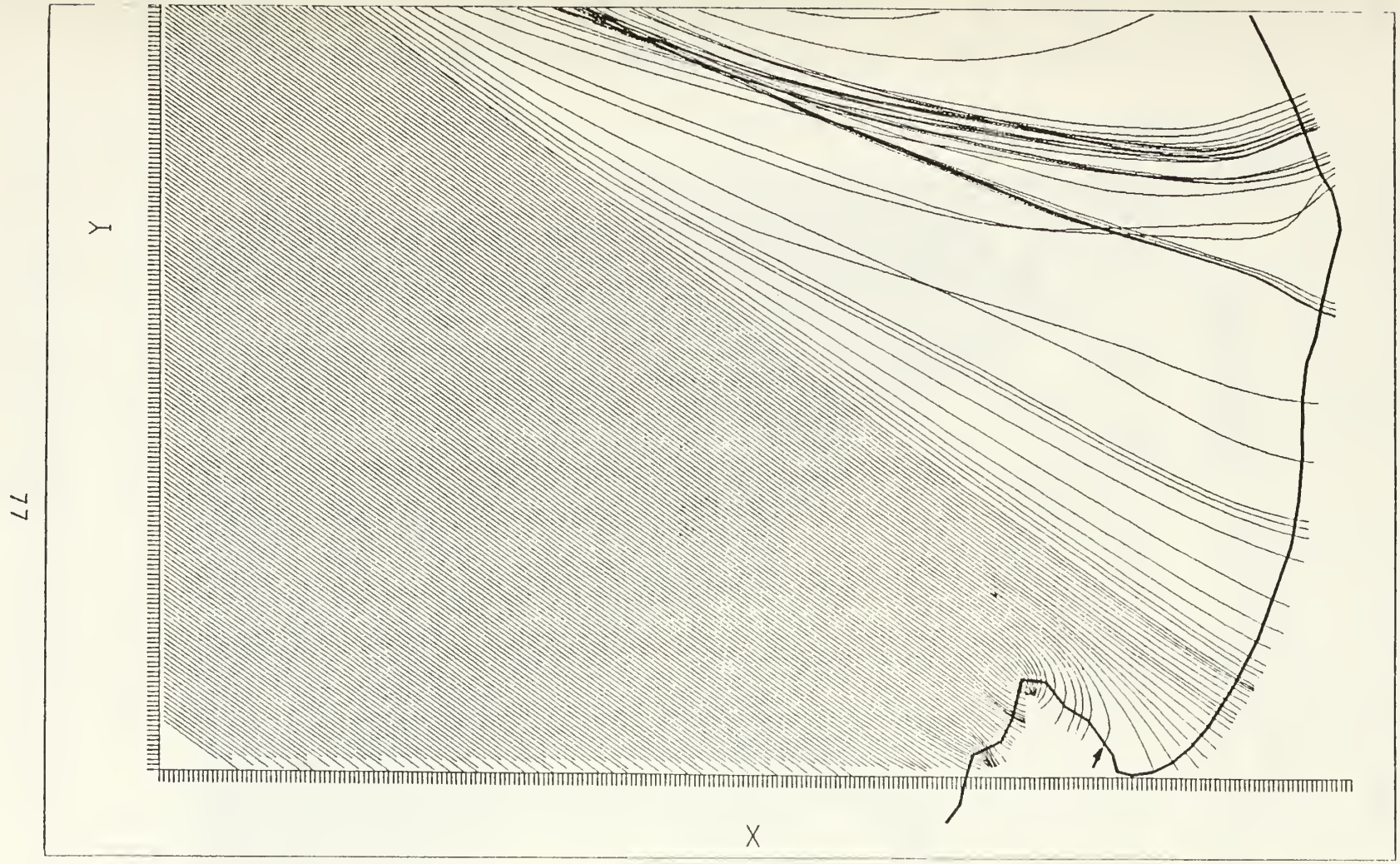

Figure 4.1 Wave Refraction Diagram (Direction: WNW , Period: 15 s)

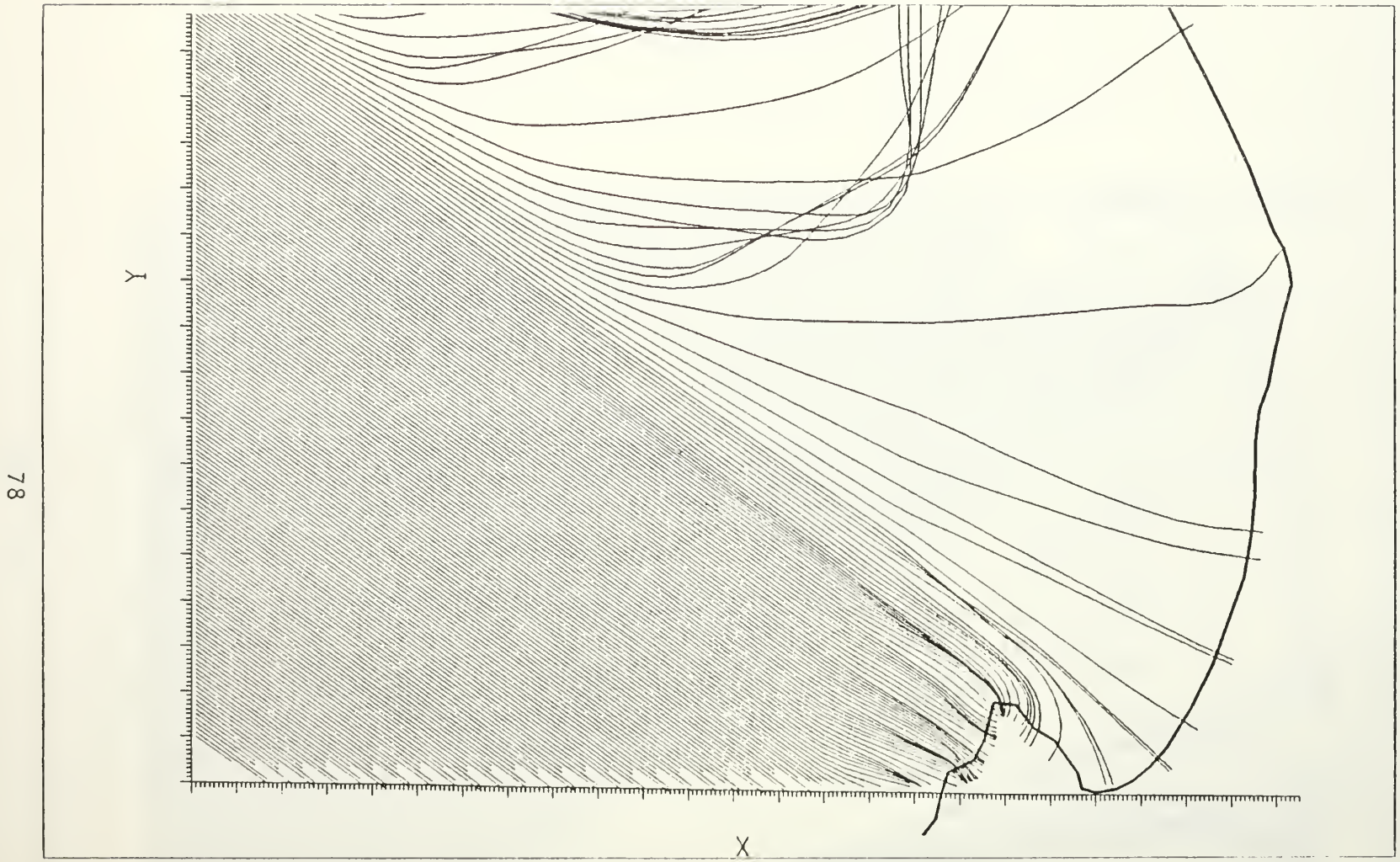

Figure 4.2 Wave Refraction Diagram (Direction: WNW, Period: 25.70 s)

By applying refraction and shoaling transformation functions to the two-dimensional deep-water wave spectrum, the shallow-water wave spectra are obtained from Equation 4.1 Waves having periods shorter than 7.5 seconds were not considered. Such short period-waves are locally generated in deep water, and experience indicates they are not representative of the short-period, locally-generated waves at the coast.

Several convenient measures can be used to describe the waves. Since the spread of angles of the shallow water wave spectra is small, it is convenient to collapse the shallow water wave specta into one-dimensional wave spectra as a function of frequency only.

$$S_h(f) = \sum_{\theta} S_h(f,\theta)\ \Delta\theta \qquad (4.5)$$

The significant wave height (the average of the highest one-third of the waves) corresponds closely to the wave height seen by an observer and is a commonly used wave statistic. Hs is calculated as a function of the total energy of the spectrum.

$$Hs = 4\left(\sum_{f} S_h(f)\ \Delta f\right)^{1/2} \qquad (4.6)$$

The modal period is the period of the spectral peak and is representative of the average period of the waves.

The speed of energy propagation is given by

$$C_g(f) = \frac{C}{2}\left[1 + \frac{2\,k\,h}{\sinh 2kh}\right] \qquad (4.7)$$

where C is the phase speed, and the wave number k is related to the frequency by

(4.8)

The wave power is recognized as an important parameter associated with beach processes. The average power per unit area is given by:

$$P = \sum_{f} E_h(f)\, C_g(f)\, \Delta f \qquad (4.9)$$

where the energy density of the waves is given by

$$E_h(f) = \rho\, g\, S_h(f) \qquad (4.10)$$

C. WAVE SET-UP AND RUN-UP

Wave set-up is the increase in mean sea level in the shoreward direction across the surf zone due to the shoreward transport of momentum by waves. The maximum set-up occurs at the shoreward limit of set-up as indicated in Figure 4.3 . The wave set-up was measured on a mild sloping beach by Guza and Thorton (1981) and found proportional to the deep water wave height. Holman and Sallanger (1983) extended the measurements for steeper beaches and a much wider range of wave heights finding similar results but with some correlation with tidal stage. For high tide conditions, the setup is given by

$$\bar{n} = 0.14 H_{s,o} \qquad (4.11)$$

where $H_{s,o}$ is the significant wave height in deep water.

Wave run-up refers to the rush of water from broken waves up the beach, and is measured by the vertical elevation reached above the still-water level. Coincident arrival with the highest high tide may cause the biggest erosion of the shoreline. The magnitude of the vertical run-up can be determined by the characteristics of the waves, by the refractive effects of the bottom topography

and by the configuration of the beach. Guza and Thornton (1981) found that in their measurements on mild beaches the vertical extent of run-up, Rv, was proportional to the deep water wave height. Again, Holman and Sallanger (1983) extended the range of measurements and suggest for high tide conditions

$$R_v = 0.88 H_{s,0} \qquad (4.12)$$

The set-up and run-up formulations will be incorporated in a simple erosion model described next.

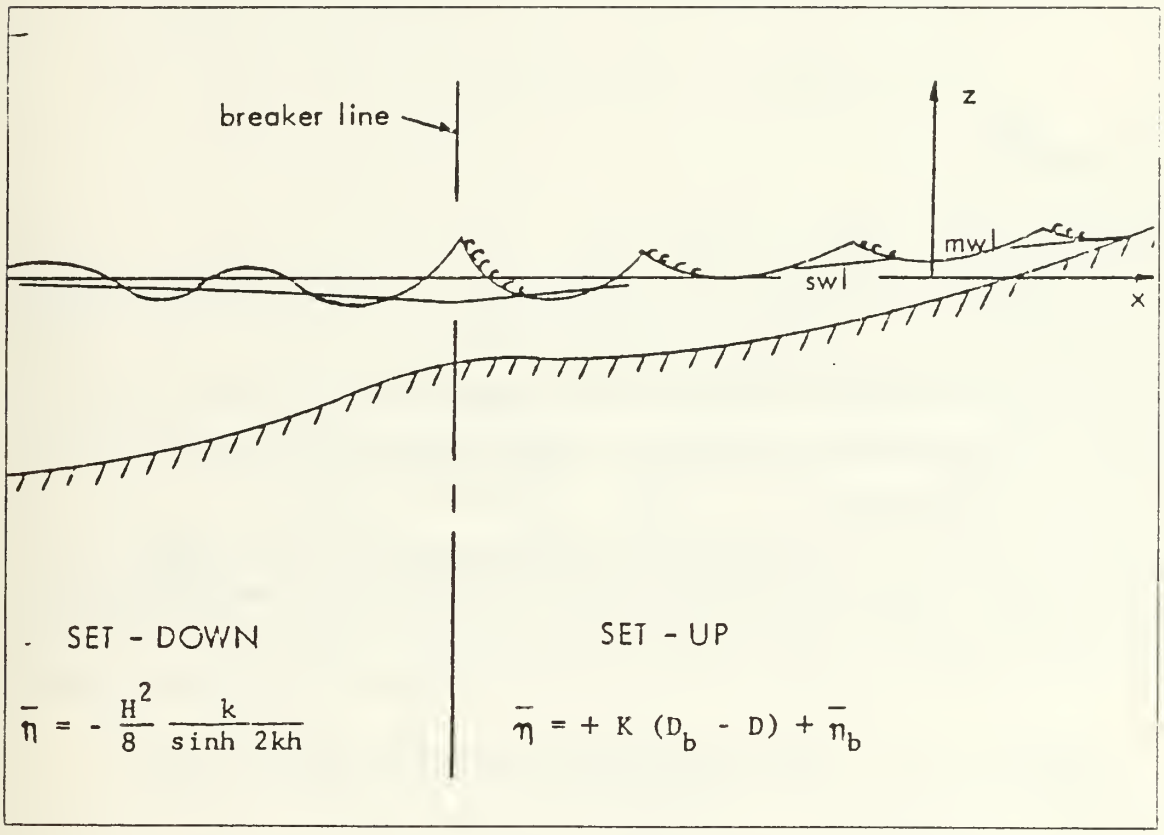

Figure 4.3 Change in Mean Water Level

V. PREDICTIVE BEACH EROSION MODEL

A. MODEL FOR BEACH PROFILE RESPONSE

A simple model is proposed here based on the hypothesis that erosion only occurs infrequently when the water elevation, S, exceeds the toe of the cliff elevation T. Each time that the total water level, S, is greater than the toe elevation, erosion can occur in the cliff (see Figure 5.1).

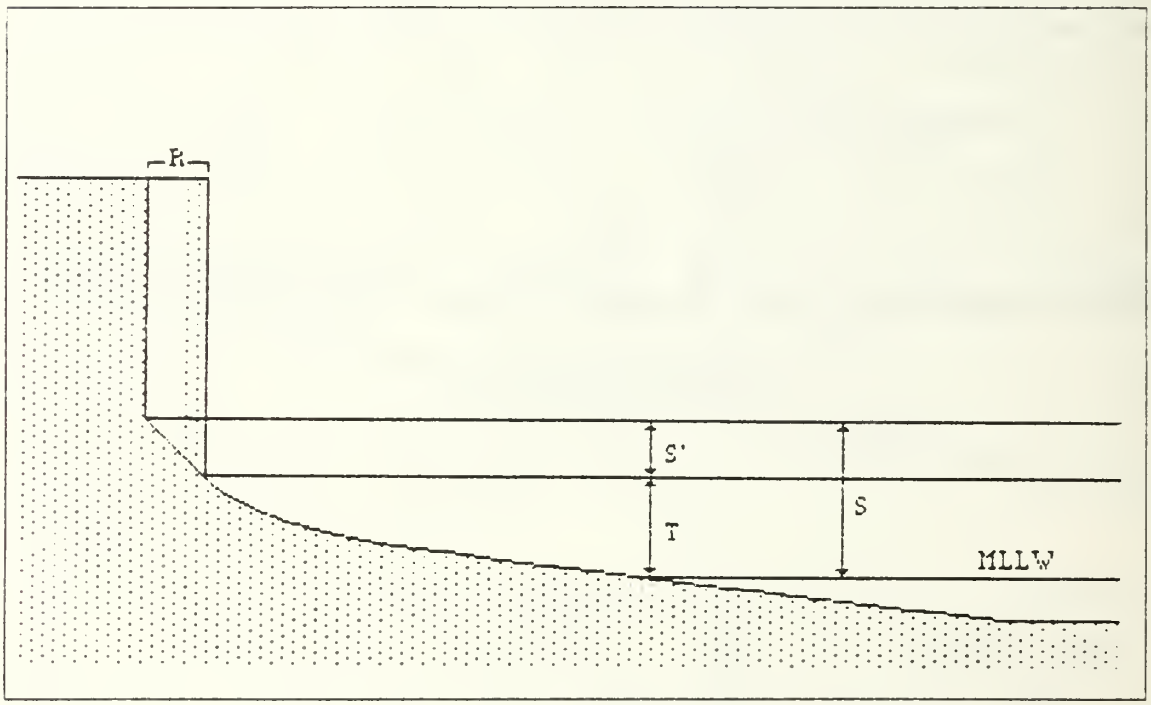

Figure 5.1 Characteristics of the response Model

The cliff recession is assumed to be given by

$$R = k\,(S'/\tan\beta) \qquad (5.1)$$

where, R, is the magnitude of the horizontal recession, β is the slope of the beach, and S' is the given by

$$S' = S - T \tag{5.2}$$

The slope for each region was calculated using the slope between the isobath contours of 0 and 2 fathoms obtained from the field sheet DA/NPGS-79. The average slopes are shown in Table 12 . The average top and toe elevations of the cliff were fcund by leveling in the study areas. The average elevations are indicated in Table 12 . The propotionality factor k accounts for differences in material and other (unknown) factors.

The total water elevation S, is calculated by

$$S = \bar{n}_{TIDE} + \bar{n} + R_V \tag{5.3}$$

where, n_{TIDE} ,accounts for the tide height above MLLW, predicted by harmonic analysis (see Chapter 3), the wave set-up, $\bar{n}$, given by equation 4.11 and the vertical extent of wave run-up, R_V, given by equation 4.12 . The wave set-up and run-up formulas are parameterized on the signficant deep water wave height, $H_{S,0}$. A corresponding deep water wave height was calculated by taking the shallow water wave height calculated in 4 meters back out into deep water without accounting for refraction assuming conservation of energy flux as follows:

$$H_{S,0} = H_{S,4M} \left(\frac{1}{K_S(f_P)}\right) \tag{5.4}$$

where fp is the peak frequency in the shallow water wave spectrum. The maximum water elevation due to tides and waves is predicted hourly for the intervals between photographs and the predicted recession using equation 5.1

summed. The predicted recession rates were obtained by application of the model, using a proportionality coefficient k = 0.000096 (see Table 4.11).

The measured and predicted recession rates for each time period (1966-1976, 1976-1978, 1978-1983) normalized by the values for the entire period (1966-1983) are compared in Figure 5.2 . The north and south recession rates for Ft. Ord, Sand Dune and Beach Lab areas are averaged to give single measured values. The results show that the model gives a reasonable indication of the temporal variability of erosion, i.e. the model predicts high erosion when the erosion was measured high during a particular time interval and vice versa

The average measured and predicted recession rates for the entire comparison interval 1966-1983 are compared in Figure 5.3 . The model predicts maximum erosion at Ft. Ord decreasing south, but predicts less erosion at Sand Dune than at Phillips Petroleum. The high measured recession rate relative to the predicted rate at the Sand Dune area suggests an anomalously high recession rate. The higher than expected recession rate may be associated with the sand mining of the beach at this location.

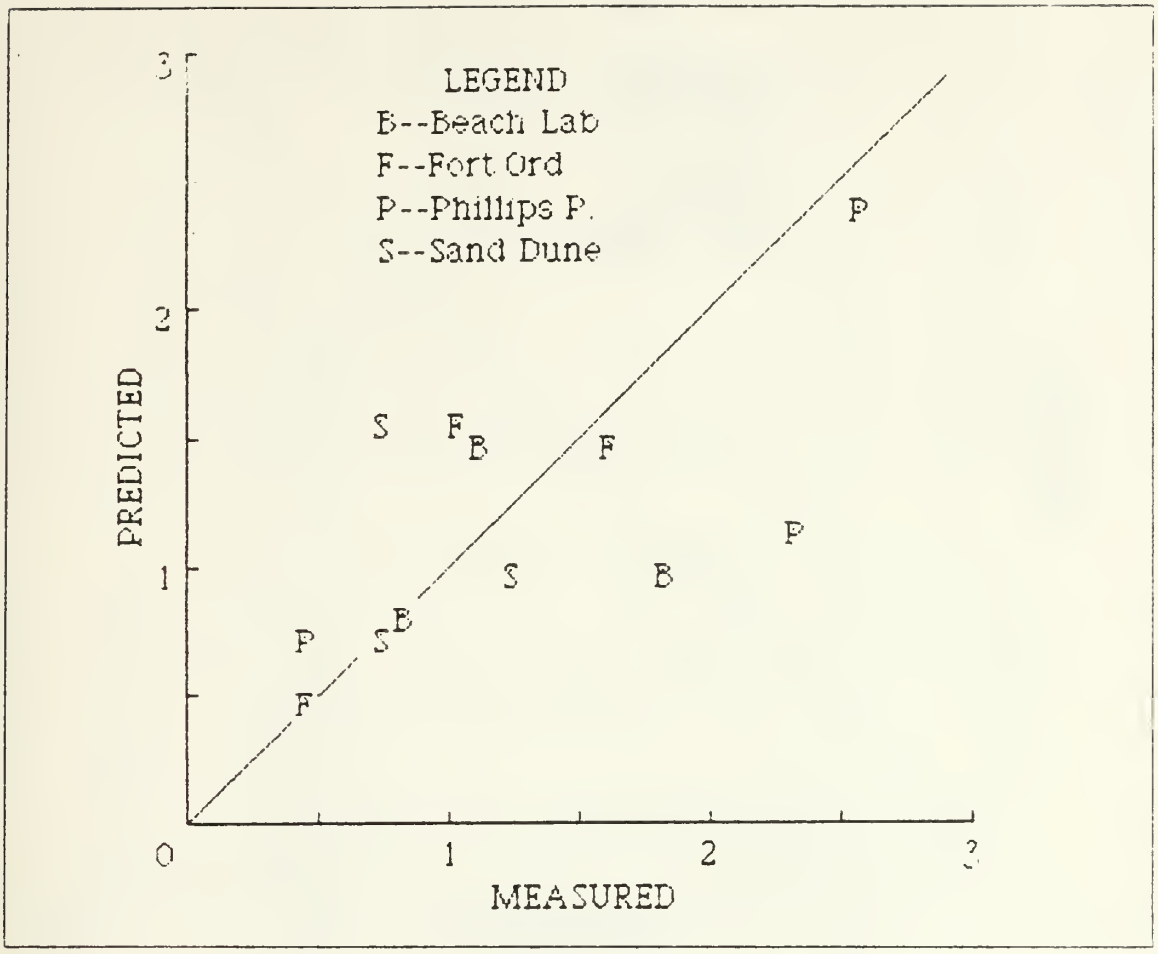

Figure 5.2 Comparison of Normalized Measured and Predicted Recession Rates

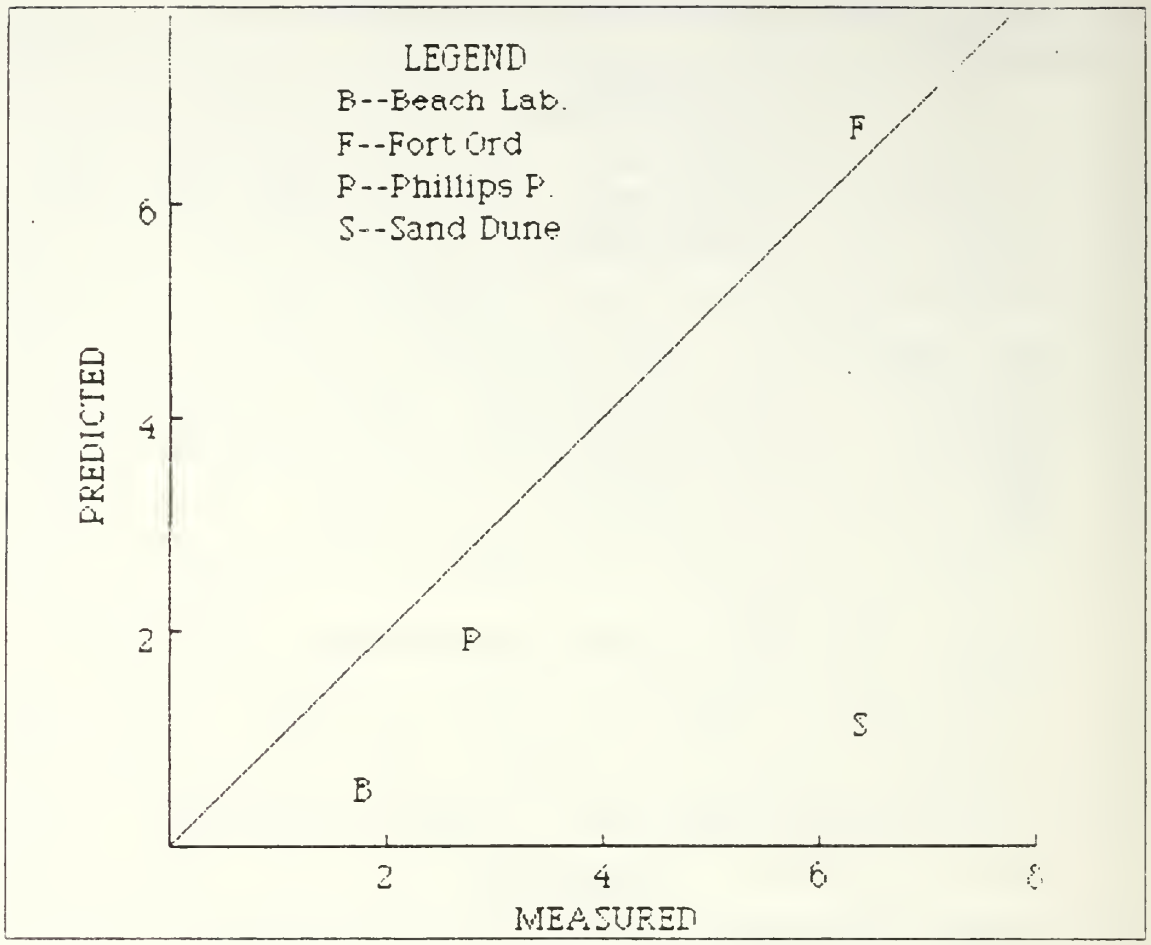

Figure 5.3 Measured vs. Predicted Recession Rates (1966-83)

TABLE 12

Characteristics of the Study Areas

LOCATION	AVERAGE NEARSHORE SLOPE	AVERAGE TOE ELEV.(MLLW) ft	AVERAGE TOP ELEV.(MLLW) ft	AVERAGE CLIFF HEIGHT ft
Beach Lab (South)	1/24	12	16	4
Beach Lab (North)	1/24	12	22	10
Phil. Petrol.	1/25	13	24	11
Sand Dune (South)	1/33	15	27	12
Sand Dune (North)	1/33	16	29	13
Fort Ord (South)	1/39	20	52	32
Fort Ord (North)	1/39	20	52	32

TABLE 13

Recession Rates given by the Model (ft/yr).

TIME INT.	1966-1976	1976-1978	1978-1983	1966-1983
LOCATION				
Ft.Ord	3.6	11.1	12.3	6.8
S. Dune	0.9	1.7	1.8	1.2
P.P.Property	1.4	4.6	2.3	2.0
B. Lab	0.5	0.6	0.9	0.6

VI. CONCLUSION

The primary objective of this study is to develop and evaluate a model for the prediction of coastal erosion rates in Southern Monterey Bay. A sequence of six aerial photographs taken during the interval 1946-1984 are used to measure coastal erosion. It is demonstrated that the aerial photographs provide a suitable means to determine coastal changes. Previous studies had not used accepted photogrammetric techniques to compensate for scale variation due to relief, parallax and plane tilt. Careful analysis was applied here to minimize errors, which is discussed in detail. Scale variations between photographs were estimated by deterimining the average scale of each photograph from horizontal ground points. Errors due to relief displacement were minimized by measuring the X-parallax of each point.

It has been shown that the top of the cliff offers a consistent measurement point for erosion studies because it is affected only by storm waves with simultaneous occurrence of high tides. It is found that the erosion along the coast of Southern Montery Bay is progressive -- there is no accretion. The average cliff top recession rate is a minimum in the southern part of the Bay and increases northward, with a maximum average erosion rate of 7.3 ft/yr (2.2 m/yr) at Fort Ord. Topographic maps combined with field surveys show that the cliff height decreases to the south.

A simple predictive model is proposed based on the hypothesis that the permanent beach erosion in Southern Monterey Bay is episodic, occurring infrequently when high tides coincide with stormy weather which allows wave action to erode the toe of the cliffs. The tides are predicted using harmonic analysis. The wave heights are calculated in

shallow-water by refracting deep water directional wave spectra provided by Fleet Numerical Oceanography Center (FNOC). Erosion occurs when the total water elevation exceeds the toe of the cliff elevation. The total water elevation is the combination of tides plus set-up and run-up, which are proportional to the wave height. The model is calibrated against the measured recession rates for the years 1966-1983 when the wave data are available. The model quantitatively predicts the temporal variability of the recession rates occurring between the aerial photograph intervals. The model reasonable predicts the spatial variation of the recession rates, indicating maximum erosion at Fort Ord and decreasing to the south. The variability in erosion is attributed to variations in the incident wave energy along the shoreline due to wave refraction.

APPENDIX A
SCALE VARIATION DUE TO TILT

The concept of a tilted photograph is presented here. Some commonly used terms for tilted photographs are illustrated in Figure A.1 .

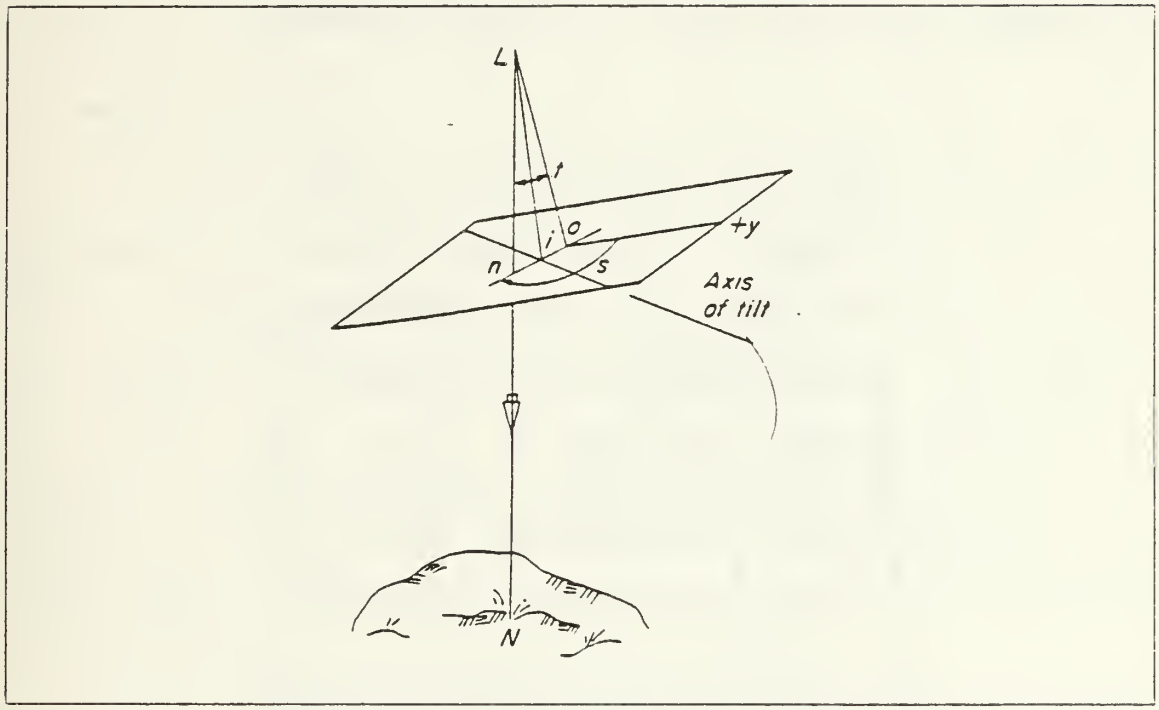

Figure A.1 Elements of Tilted Photographs

The Nadir point, n, is that point at which a vertical line through the perspective center, L, of the camera lens pierces the plane of the photograph. Tilt, t, is the angle between the vertical line and the optical axis, Lo. The isocenter, i, is the point on a photograph intersected by the bisector of the tilt angle. The isocenter is significant because it is the center of radiation for displacements

of images due to tilt. The axis of tilt is a line perpendicular to the principal line and passing through the isocenter. Swing, s, is the angle at the principal point of a photograph which is measured clockwise from the positive y-axis to the principal line at the nadir point, n,.

The effect of tilt in an aerial photograph is to cause the scale to vary throughout the picture, even if the ground is flat and level. If the scale near the center is correct, then the scale is smaller on the side that is tilted upward and larger on the side that is tilted downward.

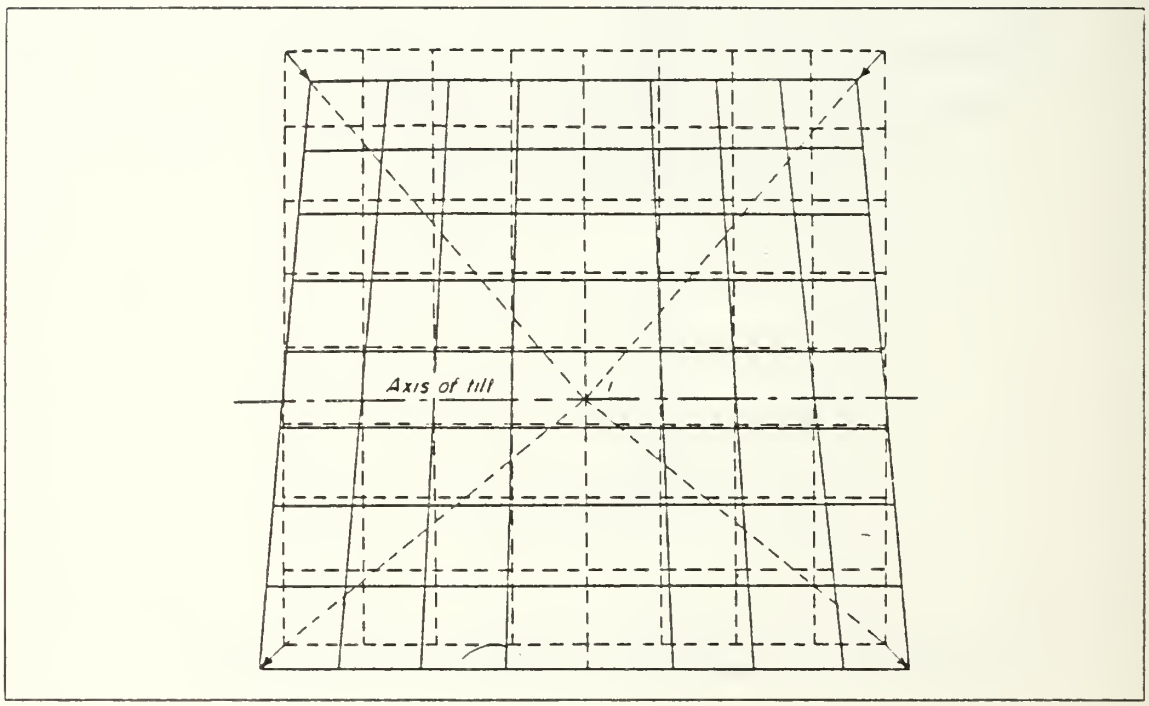

Figure A.2 Scale Variation on Tilted Photograph

This is illustrated in Figure A.2, where dashed lines represent a square grid on a flat and level ground as it would appear on a truly vertical photograph. The solid lines represent the same grid as it would appear on a photograph that has been tilted toward the upper part of the

diagram. The scale of the grid is the same on both the truly vertical and the tilted photograph only along the axis of tilt (Moffitt, 1980).

The scale of any image on a tilted photograph is given by

$$S = (f - y \sin t) / (H - h) \qquad (A.1)$$

where t is the tilt angle, y is the distance of the image from the isocenter measured in the direction of the tilt, positive on the upper side, and where the other terms have already been defined.

From Equation A.1 it is obvious that the scale depends on the amount of the tilt, the position of the image on the photograph relative to the direction of the tilt and f, H and h. Also, the magnitude of the scale variation across a tilted photograph is directly proportional to the change in the distance y of an image measured in the direction of the tilt. For tilts of less than approximately three degrees, scale variations are relatively small and can be ignored. Tilt is most objectionable where photographs are being used to determine elevations of points on the ground (Slama, 1980).

There are several methods to determine the tilt of a photograph. To compute the tilt, ground positions of three or more image points in the photograph must known. These methods are discussed in Slama (1980). The least complicated method is to rectify aerial photographs. Rectification is the process of projecting the negative of a photograph, utilizing a special projection printer, from its plane onto another plane by translation, rotation, and scale change. The negative is tilted about the two axes by computed amounts equal to the tilt of the photograph.

In the above process the rectified photographs usually are enlarged to adjust all the photographs to a common scale. After rectification of the photograph, the scale will not be further affected by the tilt.

Most agencies have specific limits on the amount of tilt permitted. The Agricultural Stabilization and Conservation Service specifies that a resultant tilt exceeding four degrees may be cause for rejection of photographs (Stafford, 1971). In case rectified enlargements are not available, the simplest method which can be utilized to reduce the error caused by scale variation due to tilt is to compute several scales by the methods referred in the previous section and calculate their average.

APPENDIX B

RECORDING OF DATA AND COMPUTER PROGRAMS

All measurements were recorded on a specially designed data sheet that included all data necessary to process the information. It was designed with the same format as the input data program. The following data are included on the recording sheet (Figure &57) : (a) Ground distance between points A and B and between C and D; (b) scale of the chart; (c) reference parallax; (d) focal length of the aerial camera; (e) year of the photograph and code of the area, i.e. Fort Ord 1978 was coded "1978fo"; (f) X- and Y- coordinates of the principal point of the left photograph; (g) X- and Y- coordinates of the principal point of the right photograph; (h)Identification of the point, X- and Y- coordinates, and X parallax of the reference points A, B, C and D; (i) identification of the points X- and Y- coordinates, and their X- parallaxes.

Upon completion of the measurement and recording of the data necessary to make a comparison of a beach location on two sets of photographs, data were processed. The calculations necessary to reduce the data were highly repetitive and ideally suited for the computer. For this purpose, three computer programs were written. The first program transformed the photo coordinates input data to ground coordinates at a scale of 1/2000. These coordinates were corrected for relief displacement using Equation 1.4; the second program plotted the reduced coordinates on a chart of dimensions 18" x 36"and the third program using linear interpolation to calculate the average rate of erosion, its standard deviation, the area eroded, and average volume eroded using an average elevation.

FILE: 1946FO DATA A1

49646.00 45110.00 2000.000

36.27 152.4 1946FONE

94.26 430.13

183.10 429.56

A	133.88	481.19	36.27
B	129.27	482.72	36.28
C	127.66	482.36	36.31
D	126.30	478.12	36.31
C1	67.80	480.64	36.70
C2	72.78	481.22	36.36
C3	78.52	482.02	36.58
C4	80.82	482.42	36.43
C5	84.54	482.76	36.43
C6	87.66	483.00	36.28
C7	89.78	483.43	36.22
C8	94.16	483.42	36.18
C9	97.46	483.72	36.08
C10	99.90	483.94	36.03
C11	104.24	484.26	35.92
C12	107.60	484.46	35.80
C13	111.54	485.07	35.70
C14	118.70	486.10	35.70
C15	123.30	486.84	35.50
C16	129.28	487.14	35.40
C17	132.48	487.66	35.37
C18	136.22	488.68	35.18
C19	141.26	488.92	35.05
C20	146.02	489.72	35.05

Figure B.1 · Recording Data Sheet

APPENDIX C
TIDE TABLES

Values for each one of the tidal constituents, having amplitude greater than 0.02 feet, are listed in Table 14 . The calculated terms for each one of the costituents are listed in Table 15 .

TABLE 14

Tidal Constituents for Monterey, California

Monterey Municipal Wharf No. 2

1 January,1974 - 31 December, 1974

Prepared by:

Tides Branch

National Ocean Survey

Constituent	H Amplitude	k Epoch	A $k'-k$	D $-k'$
M2	1.625	297.400	11.9	-309.3
S2	0.425	295.500	3.8	-299.3
N2	0.366	272.000	16.3	-288.3
K1	1.216	97.800	1.6	-99.4
O1	0.763	81.400	10.4	-91.8
ν_2	0.069	279.400	15.4	-295.1
μ_2	0.046	234.400	20.0	-254.4
(2N2)	0.046	248.500	20.6	-269.1
(OO1)	0.039	119.600	-7.2	-112.4
λ_2	0.011	296.500	8.1	-304.6
S1	0.038	202.300	1.9	-204.2
M1	0.117	114.800	5.9	-120.7
J1	0.071	107.000	-2.8	-104.4
ρ_1	0.029	74.300	14.1	-88.4
Q1	0.137	72.900	14.7	-87.6
T2	0.025	295.500	4.1	-299.6
(2Q)1	0.020	65.000	19.1	-84.1
P1	0.381	92.700	2.2	-94.9
L2	0.046	322.800	7.6	-330.4
K2	0.121	287.700	3.1	-290.8

TABLE 15

Calculated Constituent Terms for Monterey

Monterey Municipal Wharf No. 2

1 January,1974 - 31 December, 1974

Prepared by:

The Authors

Constituent	a Speed	f Node Factor	(V+u) Argument
M2	28.9841042	0.984	173.4
S2	30.0000000	1.000	-3.8
N2	28.4397295	0.988	265.7
K1	15.0410686	1.010	17.6
O1	13.9430356	1.015	151.6
ν_2	28.5125831	0.988	256.0
μ_2	27.9682084	0.988	-11.6
(2N2)	27.8953548	0.988	-1.9
(OO1)	16.1391017	1.049	71.8
λ_2	29.4556253	0.988	270.7
S1	15.0000000	1.000	178.1
M1	14.4966939	1.274	152.8
J1	15.5854333	1.023	289.4
ρ_1	13.4715145	1.015	234.0
Q1	13.3986609	1.015	244.0
T2	29.9589333	1.000	-1.9
(2Q)1	12.3542862	1.015	336.3
P1	14.9589314	1.000	347.5
L2	29.5284789	1.142	274.8
K2	30.0821373	1.006	215.1

APPENDIX D
HISTORIC OCEAN STORMS

Historic ocean storms for Monterey Bay are listed in Table 16 . They are collected from earlier studies performed by Tompson (1978) and Jones (1983).

TABLE 16

Historic Ocean Storms (Monterey Bay)

1 January,1946 - 31 December, 1983

Date-Year	Source	Direction/ Type of Storm
4 Mar. 1946	Jones	North Winds
28 Jan. 1947	Jones	Norterly Gale
4 Apr. 1947	Jones	Northerly
23 Feb. 1948	Jones	Northwest
2-3 Jan. 1949	Jones	Heavy Winds
27-29 Oct. 1950	Jones	Northerly Gale
6 Mar. 1951	Thompson	Northwest
2 Dec. 1951	Jones	Southeastern
5 Dec. 1951	Thompson	Northwest
7 Dec. 1952	Thompson	Westerly
23 Feb. 1953	Jones	Northeast Gale
13 Nov. 1953	Jones	Southerly
1 Dec. 1953	Thompson	Northeast
13 Feb. 1954	Thompson	Westerly
19 Dec. 1955	Thompson	Southwest
23 Dec. 1955	Thompson	Southwest
21 Feb. 1956	Thompson	Westerly
4 Mar. 1956	Thompson	Westerly
3 Apr. 1958	Thompson	Northwest
14 Nov. 1958	Thompson	Northwest
9-10 Feb. 1960	Jones	Southerly and Westerly
1 Feb. 1963	Jones	Northwest

Table 16
Historic Ocean Storms (Monterey Bay) (cont'd.)

7 Mar. 1964	Thompson	Northwest
28 Dec. 1965	Thompson	Southwest
24 May. 1967	Thompson	Northwest
3 Dec. 1967	Thompson	Northwest
10 Dec. 1968	Thompson	Northwest
6 Feb. 1969	Jones	-
24 Feb. 1969	Thompson	Southwest
11 Dec. 1969	Thompson	Southerly
15 Jan. 1971	Thompson	Southerly
22 Jan. 1972	Thompson	Southwest
16 Jan. 1973	Thompson	Southwest
24 Feb. 1973	Thompson	Southerly
28 Mar. 1973	Thompson	Northwest
16 Jan. 1974	Thompson	Southwest
1 Mar. 1974	Thompson	Southwest
9 Jan. 1978	Jones	South and Southwest
16 Jan. 1978	Jones	Southwest
25-27 Jan. 1978	Jones	Southwest
5 Mar. 1978	Jones	-
16-19 Feb. 1980	Jones	Southerly
1 Dec. 1982	Jones	Northwest
2 Dec. 1982	Jones	-
23 Dec. 1982	Jones	Winds up to 70 mi./hr
28 Jan. 1983	Jones	Southerly
1 Mar. 1983	Jones	Southwest

LIST OF REFERENCES

1. Bretschneider,D.E., Sea Level Variations at Monterey, California, M.S.Thesis,Naval Postgraduate School, Monterey, March 1980.

2. Flick,B.E.,and Cayan,D.R., Extreme Sea Levels on the Coast of California, paper, 1984.

3. Guza, R. T., and Thornton, E. B., Swash Oscillations on a Natural Beach, J. Geophysical Research, 87(C1), 483-491, 1982.

4. Guza, R. T., and Thornton, E. B., Wave Set-up on a Natural Beach, J. Geophysical Research, 86(C5), 4133-4137, 1981

5. Holman, R. A., and Sallenger, A. H., Setup and Swash on a Natural Beach, J. Geophysical Research,90(C1), 945-953, 1985.

6. Jones, G. B., Coastal Erosion at Selected Points on Southern Monterey Bay, Senior Thesis, University of California, Santa Cruz, July 1983.

7. Keller,M., Photogrammetry Engineering and Remote Sensing, NOS, 1975.

8. King,A.M., Beaches and Coasts, Arnold, 1959.

9. Komar,D.P., Handbook of Coastal Processes and Erosion, CRC Press , 1983.

10. Maixner, H. V., Comparison of Predicted and Observed Tides at Monterey, California, M.S.Thesis,Naval Postgraduate School, Monterey, March 1973.

11. Mohamed, T., El-Ashry, Air Photography and Coastal Problems, Dowden, Hutchinson and Ross, Inc., 1977.

12. Moffitt, F. H., Technical Report HEL-2-21, History of Shoreline Growth from Analysis of Aerial Photograps, 1968.

13. Moffitt,F.H., and Mikhail,E.M., Photogrammetry, 3d ed., Harper and Row, 1980.

14. Schureman,P., Manual of Harmonic Analysis and Prediction of Tides, United States, Government Printing Office, October 1971.

15. Slama,C. C.,(Editor-in-Chief), Manual of Photogrammetry, 4th ed.,American Society of Photogrammetry, 1980.

16. Smith, P. O., Reconnaissance Report on Coastal Erosion, at Fort Ord, U.S. Army Corps of Engineers, Miscellaneous Papers CERC-83-10, 1983.

17. Stafford, B. D., Technical Memorandum No. 36 on An Aerial Photographic Technique for Beach Erosion Surveys in North Carolina, U.S. Army Corps of Engigeers, October 1971.

18. Thompson, W. C., Report on Coast Erosion and Run-up on Phillips Petroleum Property, prepared by the author for Ponderosa Homes, Santa Clara, December 1981.

19. Thornton, E.B., Preliminary Report on Waves at Halfmoon Bay, Prepared by the author for Severson, Werson, Berke and Melchior, April 1983.

INITIAL DISTRIBUTION LIST

		No. Copies
1.	Defence Technical Information Center Cameron Station Alexandria, VA 22314	2
2.	Library, Code 0142 Naval Postgraduate School Monterey, CA 93943	2
3.	Prof. C.N.K. Mooers Department Chairman, Code 68 Department of Oceanography Naval Postgraduate School Monterey, California 93943	1
4.	Prof. E.B. Thornton, Code 68 Department of Oceanography Naval Postgraduate School Monterey, California 93943	3
5.	Prof. S.P. Tucker, Code 68 Department of Oceanography Naval Postgraduate School Monterey, California 93943	3
6.	CAPT D.E. Puccini Fleet Numerical Oceanography Center Monterey, California 93943	1
7.	LT A.J. Sklavidis Meandrou 14, New Filadelfia Athens, Greece	7
8.	CC W.R. Lima Blanco Direccion de Hidrografia y Navegacion Observatorio Cajigal-La Planicie- Urb 23 de Enero Caracas, Venezuela	5
9.	Director Naval Oceanography Division Naval Observatory 34th and Massachussets Avanue NW Washington, DC 20390	1
10.	Commander Naval Oceanography Command NSTL Station Bay St. Louis, MS 39522	1
11.	Commanding Officer Naval Oceanographic Office NSTL Station Bay St. Louis, MS 39522	1
12.	Commanding Officer Naval Ocean Research and Devalopment Activity	1

NSTL Station
Bay St. Louis, MS 39522

13. Chairman Oceanography Department — 1
U.S. Naval Academy
Annapolis, MD 21402

14. Chief of Naval Research — 1
800 N. Quincy Street
Arlington, VA 22217

15. Director (Code PPH) — 1
Defence Mapping Agency
Bldg. 56, U.S. Naval Observatory
Washington, DC 20305

16. Director (Code HO) — 1
Defence Mapping Agency Hydrographic
Topographic Center
6500 Brookes Lane
Washington, DC 20315

17. Director (Code PSD-MC) — 1
Defence Mapping School
Ft. Belvoir, VA 22060

18. Director Charting and Geodetic — 1
Services (N/CG)
National Oceanic and Atmospheric
Administration
Rockville, MD 20852

19. Chief, Program Planning, Liaison — 1
and Training (NC2)
National Oceanic and Atmospheric
Administration
Rockville, MD 20852

20. Chief, Nautical Charting Division — 1
National Oceanic and Atmospheric
Administration
Rockville, MD 20852

21. Chief, Hydrographic Surveys Branch — 1
(n/CG24)
National Oceanic and Atmospheric
Administration
Rockville, MD 20852

22. Director, Pacific Marine Center — 1
(N/MOP)
National Ocean Service, NOAA
1801 Fairview Avenue East
Seattle, WA 98102

23. Director, Atlantic Marine Center — 1
(N/MOA)
National Ocean Service, NOAA
439 W. York Street
Norfolk, VA 23510

24. IHO/FIG International Advisory Board — 1
International Hydrographic Bureau
Avenue President J.F. Kennedy
Monte Carlo, Monaco

25. Hydrographic Service — 1
Athens BST 902
Greece

26. Nelson E. L. Blanco 1
1 calle #6 Propatria
Caracas, Venezuela

27. Engineer Office 1
Department of the Army,
7th Infatry Division
Fort Ord, California 93941

28. Prof. G. Griggs 1
Department Chairman
Department of Air Sciences
University of California
Santa Cruz, California 95064

29. Mr S. Steven 1
Map and Photo Library
University of California
Santa Cruz, California 95064

30. City Engineer 1
City of Monterey
Monterey, California 93940

31. City Engineer 1
City of Sand City
Sand City, California 93955

32. Mr. T. Kendall 1
Corps of Engineers
SPNPE-W
211 Main St
San Francisco, California 94111

33. Mr. Michael O' Bryan 1
Public Works Director
City of Seaside
P.O. Box 810
Seaside, California 93955

34. Monterey County Board of Supervisors 1
P.O. Box 180
Salinas, California 93902